

Theory of Nuclear Magnetic Relaxation in Haldane Gap Antiferromagnets

Jacob Sagi^a and Ian Affleck^b

^a*Physics Department*

University of British Columbia, Vancouver, BC, V6T 1Z1, Canada

^b*Canadian Institute for Advanced Research and Physics Department*

University of British Columbia, Vancouver, BC, V6T 1Z1, Canada

(August 11, 2018)

Abstract

A Theory of Nuclear Magnetic Resonance (NMR) is developed for integer-spin, one-dimensional antiferromagnets, which exhibit the Haldane gap. We consider free boson, free fermion and non-linear σ -model approaches, all of which give similar results. Detailed anisotropy and magnetic field dependence is calculated and compared with experiment.

75.10 Jm

I. INTRODUCTION

The one-dimensional Heisenberg antiferromagnet was argued to have a gap for integer (but not half-integer) spin by Haldane¹, in 1983. Since that time a considerable amount of theoretical and experimental work has been done on this system. Many properties of this system have been calculated using relativistic quantum field theories in (1+1) space-time dimensions. While the non-linear σ -model is probably the most firmly established model for this system, only a few of its features can be calculated exactly, so other more approximate models have been used extensively, notably free boson and free fermion models. All three models are generally expected to give qualitatively similar results. These models have been used to analyze neutron-scattering, susceptibility, electron spin resonance and other experiments (see [2–8] and references therein). Our purpose here is to develop this theoretical framework to study nuclear magnetic resonance and to compare the theory to published experiments. Some of our results were obtained independently by Jolicoeur and Golinelli⁸.

We consider the general Hamiltonian for $S = 1$:

$$H = \sum_i \{ J \vec{S}_i \cdot \vec{S}_{i+1} + D(S_i^z)^2 + E [(S_i^x)^2 - (S_i^y)^2] - \mu_B \vec{H} \cdot \mathbf{G} \cdot \vec{S}_i \}. \quad (1.1)$$

For sufficiently small D/J and E/J , the model is still in the Haldane gap phase. In the pure Heisenberg model ($D = E = 0$) the lowest excited state is a triplet, at energy $\Delta \approx .4105J$ above the singlet groundstate. The D term splits the triplet into a singlet and doublet, and the E term further splits the doublet. A uniform magnetic field lowers the energy of one element of this triplet; it vanishes at a critical field, H_c . If the Hamiltonian is invariant under rotations about the field direction (eg. $E = 0$ and the field is in the z direction), then there is quasi-long-range antiferromagnetic order above H_c . If the Hamiltonian does not have this invariance, there is true long-range order above H_c . The gyromagnetic tensor, \mathbf{G} , is often assumed diagonal although we consider more general situations (see Appendix C.)

The NMR rate, $1/T_1$, is given by:

$$\begin{aligned} 1/T_1 &\propto \sum_{i,j} \int_{-\infty}^{\infty} dt e^{-i\omega_N t} A^{bi} A^{jb} \langle \{ S^i(0, t), S^j(0, 0) \} \rangle \\ &\propto \sum_{i,j} A^{bi} A^{jb} \sum_{n,m} e^{-E_n/T} (1 + e^{\omega_N/T}) \langle n | S^i(0) | m \rangle \langle m | S^j(0) | n \rangle \\ &\quad 2\pi \delta(E_n - E_m - \omega_N). \end{aligned} \quad (1.2)$$

Here A^{jb} is the hyperfine coupling between the nucleus and the Ni spin. b is the direction of the RF field. In NENP, we will generally assume that $A^{ab}(q)$ is not strongly q -dependent and is independent of b after averaging over the various nuclei. $\langle \rangle$ denotes a thermal average in an applied magnetic field, H (normally perpendicular to the RF field). $\omega_N \equiv \mu_N H$ is the nuclear Larmor frequency. This is of order $1mK$, negligibly small compared to the other relevant energy scales. Thus we are concerned with transitions between states n and m with essentially no change in energy but arbitrary change in wave-vector. We also can essentially set $e^{\omega_N/T} = 1$. We will concentrate on calculating $1/T_1$ in the low T limit, $T \ll \Delta$, the

Haldane gap, where the low energy field theory approximation may be used. In this limit, there are contributions to $1/T_1$ from $q \approx \pi$ and $q \approx 0$.

There are several facets to a calculation of the NMR rate. We must consider contributions from two different ranges of q . Furthermore, the nature of the excitations changes radically near the critical field. As we vary the field at fixed temperature, we may identify three different regions: $\mu_B(H_c - H) \gg T$, $\mu_B|H - H_c|$ of $O(T)$, and $\mu_B(H_c - H) \ll T$. The behaviour of $1/T_1$ is quite different depending on whether or not there is rotational symmetry around the direction of the static field. Finally, the presence of defects, ie. chain ends, may lead to additional structure at temperatures well below Δ .

In this paper, we mainly focus on the regime $\mu_B(H_c - H) \gg T$, $\Delta \gg T$. In the rotationally invariant case, we give an asymptotically exact expression for the rate which is quite independent of any detailed assumptions underlying the field theories. Without rotational symmetry more complicated and somewhat model-dependent expressions are obtained. In both cases $q \approx 0$ dominates at low T . Our result in the isotropic, zero field limit, was obtained previously by Jolicoeur and Golinelli⁸.

We also give a partial analysis of the region where $\mu_B(H_c - H) \ll T$. We show that the free fermion model gives an exact description of this region, for $q \approx 0$, with or without axial symmetry. We also consider $q \approx \pi$ in this field region, showing that it actually dominates over $q \approx 0$.

Where possible we compare our results to the experiments of Fujiwara et al.⁹ on $\text{Ni}(\text{C}_2\text{H}_8\text{N}_2)_2\text{NO}_2(\text{ClO}_4)$ (NENP). While the overall agreement is fairly good, one puzzling discrepancy is encountered.

In Sec. II we briefly review the field theory treatment of this system and estimate the size of the $q \approx \pi$ and $q \approx 0$ contributions to $1/T_1$. In particular, we review and generalize arguments that the free fermion model should become exact near the critical field. Sec. III considers the contributions to $1/T_1$ below the critical field for the isotropic and anisotropic cases. Sec. IV partially analyzes the region near criticality. Appendix A contains the details of the model calculations. Appendix B suggests a possible additional contribution to $1/T_1$ at low fields and low temperature. We expect the presence of non-magnetic defects, which essentially break up the system into finite length chains, to have a radical effect on the low energy properties of the system. Essentially decoupled $S = 1/2$ degrees of freedom appear at each chain end. This mechanism is not in itself sufficient to fully explain the low field experimental data. Finally, appendix C makes note of structural properties of NENP which are expected to have effects on experiment.

II. OVERVIEW

At least three different field theories have been used extensively to discuss Haldane gap antiferromagnets. The first, and probably best founded is the non-linear σ -model¹. The antiferromagnetic order parameter, is represented by a three-component field, $\vec{\phi}$, obeying a constraint, $\vec{\phi}^2 = 1$. The uniform magnetisation density is represented by the conserved density, \vec{l} , of the field theory:

$$\vec{l} \equiv (1/vg)\vec{\phi} \times \partial\vec{\phi}/\partial t. \quad (2.1)$$

Thus the spin operator at site i is written:

$$\vec{S}_i \approx s(-1)^i \vec{\phi} + \vec{l}, \quad (2.2)$$

and the Heisenberg Hamiltonian density as:

$$\mathcal{H} \approx \frac{vg}{2} \vec{l}^2 + \frac{v}{2g} \left(\frac{d\vec{\phi}}{dx} \right)^2. \quad (2.3)$$

This is expected to give the asymptotic low-energy long-distance behaviour of the Heisenberg model at large, integer-valued spin magnitude, s . The spin-wave velocity and coupling constant are given (up to higher order in $1/s$) by:

$$v = 2Js, g = 2/s. \quad (2.4)$$

Due to strong quantum fluctuations in one dimension, the groundstate is a (disordered) singlet and there is a gap, Δ to the lowest excited states, a triplet. For large s ,

$$\Delta \propto J e^{-\pi s}. \quad (2.5)$$

(In the half-integer s case, an additional topological term must be added to the Lagrangian, leading to gapless behaviour.) The staggered spin field, $\vec{\phi}$, acting upon the groundstate, produces the triplet of single-particle states. However, the uniform magnetisation field, \vec{l} , is a two-magnon operator, producing or annihilating a pair, or else flipping the polarization of a magnon. Hence the low temperature neutron scattering cross-section is dominated by single magnon production for wave-vector q near π and by two-magnon production for q near 0.

Unfortunately, relatively little exact information is available about the σ -model. Exact S-matrix results indicate that the spectrum consists purely of the triplet of magnons, together with multi-particle scattering states but no boundstates. The exact matrix element of \vec{l} between vacuum and two-magnon states is also known and can be used to predict the $T = 0$ neutron-scattering cross-section at small q and energies between 2Δ and 4Δ (where 4-magnon production becomes possible). It is possible to add additional terms to the Hamiltonian, reflecting the crystal field anisotropy:

$$\mathcal{H} \rightarrow \mathcal{H} + a(\phi^z)^2 + b[(\phi^x)^2 - (\phi^y)^2]. \quad (2.6)$$

However, no exact results are available on this model. Results are available from the large- n and related self-consistent approximations. In these approximations, the fields, ϕ^a , essentially become free fields with self-consistently determined masses and repulsive interactions which are assumed weak [of $O(1/n)$].

The free, or weakly interacting boson model, sometimes referred to as the quantum Landau-Ginsburg model², is obtained by relaxing the non-linear constraint, $\vec{\phi}^2 = 1$ and writing a simple $\vec{\phi}^4$ Hamiltonian:

$$\mathcal{H} = \frac{v}{2} \vec{\Pi}^2 + \frac{v}{2} \left(\frac{d\vec{\phi}}{dx} \right)^2 + \frac{1}{2v} \sum_{a=x,y,z} \Delta_a^2 \phi_a^2 + \lambda |\vec{\phi}|^4. \quad (2.7)$$

Here the Δ_a are phenomenological mass terms, giving the gaps, which can be given different values for each of the three components, ϕ^a , to model crystal field anisotropy. A phenomenological $|\vec{\phi}|^4$ term is included, when needed for stability, but is treated perturbatively.

A third, free (or weakly interacting) fermion model has quite a different motivation and is not obviously related to either of the above field theories³. The Hamiltonian is written in terms of a triplet of Majorana (ie. Hermitean) fermion fields, $\vec{\psi}_L$ and $\vec{\psi}_R$. Here L and R label left and right-moving components. The Hamiltonian density is:

$$\mathcal{H} = \frac{1}{2} \left[\vec{\psi}_L i v \frac{d}{dx} \cdot \vec{\psi}_L - \vec{\psi}_R i v \frac{d}{dx} \cdot \vec{\psi}_R + i \sum_a \Delta_a (\psi_{Ra} \psi_{La} - \psi_{La} \psi_{Ra}) + \lambda (\vec{\psi}_L \times \vec{\psi}_L) \cdot (\vec{\psi}_R \times \vec{\psi}_R) \right]. \quad (2.8)$$

Rather than being based on the large- s approximation, it appears to be special to the case $s=1$. It presumably becomes exact for the Heisenberg model with an additional isotropic biquadratic exchange interaction chosen to have the precise value to make the Haldane gap vanish¹⁰. (This model is on the phase boundary separating the Haldane and spontaneously dimerized phases.) This model has been shown to be equivalent to a $k = 3$ Wess-Zumino-Witten (WZW) non-linear σ -model, or equivalently, three decoupled critical Ising models. The critical Ising model in turn, is essentially equivalent to a massless free Majorana (ie. hermitian) fermion. Reducing the biquadratic coupling moves the Ising models away from their critical point, corresponding to adding mass terms for the fermions. Four fermion interaction terms also appear, as written above, but these are generally ignored or treated perturbatively, in a similar phenomenological spirit to that of the Landau-Ginsburg boson model. In this representation, the uniform magnetisation density, \vec{l} is again quadratic in the fundamental fields:

$$\vec{l} = \frac{-i}{2} (\vec{\psi}_L \times \vec{\psi}_L + \vec{\psi}_R \times \vec{\psi}_R). \quad (2.9)$$

The particles created by the fields, $\vec{\psi}$ are identified as magnons with masses Δ_i . We see that \vec{l} is again a two-magnon operator. It is also possible to represent the staggered magnetisation, $\vec{\phi}$ in this approach, but it is considerably more complicated. Near the massless point, this operator reduces to the fundamental field of the WZW model, or equivalently to products of the order and disorder fields, $\vec{\sigma}$ and $\vec{\mu}$ of the three Ising models. These operators are non-local with respect to the fermion fields. The corresponding correlation functions can be expressed in terms of products of Pain-Levé functions. They exhibit poles at the fermion masses together with additional structure at higher energy. Unlike in the free boson model, a simple interpretation of the staggered magnetization density as a single magnon operator doesn't hold.

To summarize, all three models have a triplet of massive magnons. In the first two models these are bosons and in the last fermions. In all models the uniform magnetisation density, \vec{l} , is a two magnon operator. In the free boson or fermion models this is exact; including interactions in any of the models we expect some contribution from 4 or more magnons. In the free boson model the staggered magnetization, $\vec{\phi}$, is purely a single magnon operator. Including interactions there is an admixture of 3 and more magnons. Recent numerical work

indicates that this admixture is very small¹¹. This operator has a complicated representation, non-local in the fermionic magnon fields, in the fermion model.

We will be concerned with adding a magnetic field to the Hamiltonian. If the associated magnetization is conserved, then the effect is rather simple. This would occur, for example, if the field is in the 3 direction and rotational symmetry about the 3 axis is a good symmetry; ie. $\Delta_1 = \Delta_2$. Consistency demands that, in any of the field theories, we couple the field to the conserved density, \vec{l} :

$$\mathcal{H} \rightarrow \mathcal{H} - g\mu_B \vec{H} \cdot \vec{l}. \quad (2.10)$$

If the associated magnetization is not conserved, then extra terms could be added¹². We will use the term in Eq. (2.10) for simplicity. In the case where the magnetization is conserved, the energy of any state is simply shifted proportional to its magnetization, m , $E \rightarrow E - g\mu_B H m$. In particular, the magnon energy gaps become:

$$\begin{aligned} \Delta_3(H) &= \Delta_3 \\ \Delta_{\pm}(H) &= \Delta_1 \pm g\mu_B H. \end{aligned} \quad (2.11)$$

Here the last two magnon eigenstates are created by the fields $\phi_1 \pm i\phi_2$. If the magnetization is not conserved then the field dependence of the energies becomes model dependent. Explicit formulas for magnon energies, $E_a(k, H)$, have been derived in free boson and fermion models⁷. The fermion result seems to agree very well with experiment; the boson one less so. As the field increases one of the gaps decreases, eventually reaching zero at a critical field of $H \sim O(\Delta/g\mu_B)$.

At low temperatures, we expect the nuclear magnetic relaxation to be dominated by q near 0 or q near π since this is where the lowest energy processes occur. It is clear that $1/T_1$ will vanish exponentially as $T \rightarrow 0$ since there is a gap. We wish to investigate whether the dominant contribution comes from $q \approx 0$ or $q \approx \pi$. Let us first use the boson model to consider $q \approx \pi$. From Eq. (1.2), we see that:

$$\begin{aligned} 1/T_1 \propto \sum_{b,i} A^{bi} A^{ib} \sum_{n,m} e^{-E_n/T} \left(1 + e^{\omega_N/T} \right) < n | \phi^i | m > < m | \phi^i | n > \\ \delta(E_n - E_m - \omega_N). \end{aligned} \quad (2.12)$$

Note that the expression is diagonal in spin operators. This is because we only consider Hamiltonians that have at least $Z_2 \times Z_2 \times Z_2$ symmetry. Any correlators which contain cross terms of spin operators will be odd under some Z_2 operation and must therefore vanish.

We assume that the magnetic field is well below H_c . As we have mentioned above, the staggered magnetization field, $\vec{\phi}$ is a single magnon operator in the non-interacting boson model. Thus it only has matrix elements between states whose energies differ by a magnon energy, $E_a(k, H)$. In particular, there is no matrix element with energy difference ω_N (which is essentially zero). Including interactions in the boson model (as for instance given by the NL σ model) there will be a contribution from $q \approx \pi$ at finite T . The simplest process is shown in Fig. 1. It involves a ϕ^4 interaction such as occurs in the quantum Landau-Ginsburg or NL σ models. The vertical line represents the field ϕ . The incoming line from the right represents a thermally excited magnon of non-zero momentum, k , and energy 2Δ . (For

simplicity, we consider the isotropic model, at zero field.) The two outgoing lines to the left represent magnons at rest. This diagram gives a non-zero matrix element proportional to λ/Δ^2 . Note however, that since the energy of the initial and final state must be at least 2Δ , there will be a Boltzmann suppression factor of $e^{-2\Delta/T}$ in Eq. (1.2). Thus the contribution to $1/T_1$ will be proportional to:

$$1/T_1 \propto \lambda^2 e^{-2\Delta/T}. \quad (2.13)$$

Including anisotropy and a finite field, there will be various contributions of this type. It remains true that all these processes are suppressed by $\exp[-2\Delta_{\min}(H)/T]$, where $\Delta_{\min}(H)$ is the minimum gap. It is also possible to interpret this calculation as giving a finite width to the single magnon state at finite T. However, this cannot change the conclusion that there is a double exponential suppression factor, contrary to the proposed model in Ref. (9).

Let us now consider contributions to $1/T_1$ from $q \approx 0$. These are given by:

$$1/T_1 \propto \sum_{b,i} \int_{-\infty}^{\infty} dt A^{bi} A^{ib} e^{-i\omega_N t} \langle \{l^i(0,t), l^i(0,0)\} \rangle. \quad (2.14)$$

There is now, in general, a contribution even in the non-interacting boson or fermion model. This comes from the terms in l^b which annihilate one magnon and create one magnon. In the presence of anisotropy, the three magnon branches are split, so we must distinguish inter-branch and intra-branch transitions (see Fig. 2). Note that both are possible since the wave-vector need not be conserved in the transition. However, the Boltzmann factor will be smaller for the inter-branch transition. In this case the optimum situation corresponds to a transition from a lowest branch magnon with a large kinetic energy to a middle branch magnon with zero kinetic energy. The Boltzmann factor is then $\exp[-\Delta_{\text{middle}}/T]$. Intra-branch transitions, in order to approximately conserve energy, will either have essentially zero change in wave-vector (forward scattering) or else the wave-vector will be essentially reversed (backscattering). Clearly the dominant process will be the intrabranched transition for the lowest branch near the minimum energy $k \approx 0$. The Boltzmann factor is now $\exp[-\Delta_{\min}/T]$. This contribution will be discussed in detail in the next section.

We now wish to discuss the behaviour near and above the critical field. Clearly once we are sufficiently close to H_c that the lowest gap is of $O(T)$, the previous analysis breaks down. The $q \approx \pi$ part may become comparable or even larger than the $q \approx 0$ part. We also need to consider possible infrared divergences and multi-magnon contributions. The nature of the critical point was established in Ref. (4). If we assume exact rotational symmetry around the field direction (which is approximately true in NENP when the field is in the chain direction) then the phase transition is in the two-dimensional xy universality class, corresponding to Bose condensation of the lowest branch of bosons. There is quasi-long-range order for the staggered moment perpendicular to the field direction above H_c , and an associated gapless mode. Without axial symmetry, the phase transition is in the 2-dimensional Ising universality class; there is true long-range-order above H_c , with the correlation length and inverse gap only diverging right at H_c .

Rather remarkably, the free fermion model gives the exact critical behaviour of the uniform part of the spin operator, with or without axial symmetry. An argument for this, in the axially symmetry case, was given in Ref. (4) [See also Ref. (13).] This follows from

the fact that the many body wave-function for a very dilute gas of repulsive bosons is just a free fermion wave-function multiplied by a sign function to correct the statistics. It is also fairly easy to see that the free fermion model becomes exact without axial symmetry. This follows from the well-known equivalence of the Ising model and a free Majorana fermion near the critical point. We emphasize that the free fermion model is certainly not exact far from H_c (although comparison with experiment indicates that it works well). Magnon interaction terms such as that in Eq. (2.8) must be included in general. However, they become irrelevant near H_c . This is quite easy to see in the Ising case. Two of the three branches of Majorana fermions remain gapped at the critical point and can be integrated out. Various interaction terms will be generated in the effective Hamiltonian for the remaining gapless fermion. However, there are no relevant interactions possible for a Majorana fermion since $\Psi_L\Psi_L\Psi_R\Psi_R$ vanishes by fermi statistics. Thus we can easily calculate the $q \approx 0$ part of $1/T_1$ right through the critical point. This is done in Section IV. The $q \approx \pi$ part is more difficult since it requires correlation functions for the 2-dimensional Ising order and disorder variables away from the critical point on a cylinder of radius $1/T$. A more sketchy discussion of this contribution is also given in Sec. IV. It turns out that the $q \approx \pi$ part dominates very close to H_c . Well above H_c , in the axially non-symmetric case, when the gap becomes larger than T again, it is simpler to use the weakly interacting boson model, as discussed in Ref. (4), to calculate the staggered part.

III. NMR RATES BELOW H_C

A. T_1^{-1} With Axial (or $SU(2)$) Symmetry: Universality of Result, Exact Sigma Model Result.

We first consider the isotropic case with the uniform magnetic field in the z -direction and the RF field in the x -direction. If the hyperfine couplings are also isotropic, $A^{ab} \propto \delta^{ab}$, then the intrabranh process doesn't occur. This follows because the RF field is perpendicular to the static magnetic field, so $1/T_1$ involves only matrix elements of S^\pm . Since the three magnon branches have definite values of $S^z = -1, 0, 1$, S^\pm can only produce interbranch transitions. For more general hyperfine couplings, there will also be a contribution from S^z . Defining,

$$S_q^z = \frac{1}{N} \sum_x e^{-iqx} S^z(x) \quad (3.1)$$

we see that in this case the leading low temperature relaxation rate will be determined by $\langle k+q, -|S_q^z|k, - \rangle$ and $\langle k+q, -|S_{q+2k}^z| -k, - \rangle$. $|k, - \rangle$ denotes the state on the lowest branch with wave-vector k and $s^z = 1$. Here q must be very small since $\omega_-(k+q) - \omega_-(\pm k) = \omega_N$. At low T , k must also be quite small since the Boltzmann factor is $\exp(-\omega_-(k)/T)$. Since the total z component of spin remains a good quantum number in the presence of the magnetic field, it follows that for $k \approx 0$,

$$\langle k, -|S^z(0)|k, - \rangle = 1 \quad (3.2)$$

where we've chosen the following measure for the one particle states,

$$\langle k|k' \rangle = 2\pi\delta(k - k'). \quad (3.3)$$

(This is true for arbitrary field, H .) In this case we can give a model independent, exact result for the low T relaxation rate. We also need the dispersion relation for the lowest branch at small k . By analyticity in k this must have the form:

$$\omega_-(k) = \Delta - h + (vk)^2/2\Delta + O(k^4), \quad (3.4)$$

where Δ is the zero field gap of the $S^z = \pm 1$ branches and we may regard this formula as a definition of v ; for convenience, we define

$$h \equiv g\mu_B H. \quad (3.5)$$

In the Lorentz invariant field theory models, we have:

$$\omega_-(k) = \sqrt{\Delta^2 + (vk)^2} - h, \quad (3.6)$$

consistent with this form. Thus we obtain from (1.2) the following expression for intrabranh relaxation along the lowest branch:

$$\begin{aligned} (1/T_1)_{\text{Intra}} &\propto 4\pi|A^{xz}|^2 \int \frac{dk dq}{(2\pi)^2} \delta(\omega_-(k+q) - \omega_-(k) - \omega_N) \\ &\times e^{-\omega_-(k)/T} |\langle k+q, -|S^z(0)|k, - \rangle|^2 \end{aligned} \quad (3.7)$$

$$\approx \frac{4|A^{xz}|^2 \Delta e^{-(\Delta-h)/T}}{\pi v^2} \int_0^\infty \frac{dk}{\sqrt{k^2 + 2\omega_N \Delta/v^2}} e^{-(vk)^2/2\Delta T} \quad (3.8)$$

The square root in the denominator of Eq. (3.8) comes from integrating over the delta function. Note that it is necessary to keep $\omega_N \neq 0$ in this equation since otherwise there is a divergence at $k \rightarrow 0$, from the diverging density of states at the gap.

At low fields, there will be interbranch transitions between the weakly split branches as well as intrabranh contributions from states with the “+” quantum number. The Boltzmann suppression will always be that of the higher branch. The most important of these subdominant contributions comes from intrabranh transitions along the “+” branch. The reason is that low momentum transitions can occur in these processes causing a square root factor as in Eq. (3.8) to be of order ω_N/v , ie. close to where the density of states diverges. The momentum transfer in the interbranch transitions must be essentially greater than the gap between the branches. The intrabranh transition rate along the “+” branch is identical to Eq. (3.8), albeit with $h \rightarrow -h$ in the exponential.

In the regime of interest, $\omega_N \ll T \ll \Delta$, Eq. (3.8) gives:

$$(1/T_1)_{\text{Intra}} \propto |A^{xz}|^2 \frac{4\Delta}{\pi v^2} [\log(4T/\omega_N) - \gamma] (1 + e^{-2h/T}) e^{-(\Delta-h)/T} \quad (3.9)$$

where $\gamma = 0.577216\dots$ is Euler’s constant. Essentially this formula, at $h = 0$, was given independently by Jolicoeur and Golinelli⁸, based on the large- N approximation to the $NL\sigma$ model. A similar expression was also derived by Troyer et. al. for the Heisenberg ladder problem having an excitation spectrum identical to the isotropic model discussed here¹⁴.

The present derivation shows that it is an exact result at $T \rightarrow 0$. We note that weak interchain couplings, J' , would also cut off this infrared divergence, replacing ω_N in the above expression by a quantity of order $\sqrt{JJ'}$.

Interbranch transitions will correspond to matrix elements

$$| \langle k+q, \pm | S^x(0) | k, 0 \rangle |^2 = | \langle k+q, \pm | S^y(0) | k, 0 \rangle |^2 \approx \frac{1}{2} \quad (3.10)$$

k and q are assumed small. The expression for the relaxation rate is identical to Eq. (3.7) with the appropriate matrix elements substituted and the energy of the higher branch in the exponential. Energy conservation enforced by the delta function will now replace ω_N by $h(1 + \frac{h}{2\Delta})$ in Eq. (3.8). One also needs to multiply the result by an overall factor of two corresponding to exchanging the labels of the states in the trace. The result is

$$(1/T_1)_{\text{Inter}} \propto (|A^{xx}|^2 + |A^{xy}|^2) \frac{4\Delta}{\pi v^2} \left[\log \left(\frac{4T}{h(1 + \frac{h}{2\Delta})} \right) - \gamma \right] (e^{-h/T} + e^{-2h/T}) e^{-(\Delta-h)/T} \quad (3.11)$$

Writing:

$$1/T_1 = (1/T_1)_{\text{Intra}} + (1/T_1)_{\text{Inter}} \equiv F(h, T) e^{-(\Delta-h)/T} \quad (3.12)$$

following Fujiwara et. al.⁹; we see that $F(h, T)$ decreases rapidly with h until $h \approx T$ at which point the effects of the upper branches disappear.

At somewhat higher T , the k dependence of the matrix elements will become important, as will the interbranch transitions. In the free boson model intrabranch matrix elements are, in fact, independent of h and identical for forward and backward scattering:

$$\langle \pm k, - | S^z(0) | k, - \rangle \approx \langle \pm k, - | l^z(0) | k, - \rangle = 1 \quad (3.13)$$

The interbranch matrix elements (corresponding to transitions $- \leftrightarrow 0$ and $+ \leftrightarrow 0$) will be

$$| \langle k, \mp | S^\pm | k', 0 \rangle |^2 \approx \frac{1}{2} \left[\sqrt{\frac{\omega'_{k'}}{\omega_k}} + \sqrt{\frac{\omega_k}{\omega'_{k'}}} \right]^2 \quad (3.14)$$

where $\omega_k = \sqrt{(vk)^2 + \Delta^2}$, $\omega'_{k'} = \sqrt{(vk')^2 + \Delta_0^2}$ and Δ_0 is the gap to the $S^z = 0$ branch (see the appendices for more details). Note that this result is still independent of the sign of k .

In the free fermion and $NL\sigma$ models the expression for backward scattering is somewhat modified:

$$\langle -k, - | S^z(0) | k, - \rangle = G(\theta) \quad (3.15)$$

The fermion model gives

$$G(\theta) = -i\Delta/\omega_k \quad (3.16)$$

while in the $NL\sigma$ model one gets

$$G(\theta) = \frac{\pi^2}{2\theta} \frac{(\theta - i\pi)}{(\theta - i2\pi)} \tanh(\theta/2) \quad (3.17)$$

where the rapidity variable, θ is given by

$$\cosh(\theta) = -1 - \frac{2v^2 k^2}{\Delta^2} \quad (3.18)$$

Note that these are still independent of h . For $vk \ll \Delta$, $\theta = i\pi + \frac{2vk}{\Delta}$, and

$$G(\theta) \approx 1 - \left(\left(\frac{2}{\pi}\right)^2 + \frac{1}{3}\right)(vk/\Delta)^2 \quad (3.19)$$

This is effectively due to magnon interactions and will, in turn, contribute a subleading T dependence to the prefactor, $F(h, T)$. Estimating the strength of the magnon interactions from experimental measurements of $1/T_1$ would be difficult, due to various other sources of temperature dependence.

Interbranch transitions in the fermion model are also sensitive to the sign of the scattering direction:

$$| \langle \pm k, -|S^+|k', 0 \rangle |^2 \approx \frac{\Delta_0^2}{2\omega_k \omega'_{k'}} \left[\sqrt{\frac{\omega_k \mp k}{\omega'_{k'} + k'}} + \sqrt{\frac{\omega_k \pm k}{\omega'_{k'} - k'}} \right]^2 \approx | \langle \pm k, +|S^-|k', 0 \rangle |^2 \quad (3.20)$$

Notice that those interbranch transitions matrix elements which contribute to $1/T_1$ are h dependent in all cases. This comes from the constraint $\omega_{\pm}(k) = \omega_0(k')$.

Actually, all of the above arguments still hold with only $U(1)$ symmetry when the field is along the symmetry direction. In principal, the function $G(\theta)$ will remain independent of field but depends on how the $SU(2)$ symmetry is broken down to $U(1)$. It is important to emphasize the universality of the leading term at low T . The only requirement is that the system possess $s_z = \pm 1$ degenerate low lying states with dispersion relation, $\omega \sim \Delta + \frac{v^2 k^2}{2\Delta}$ as $k \rightarrow 0$. Once again, the addition of hS^z to the Hamiltonian will not change the matrix elements of l^z . The new energies will be $\omega \pm h$, and with the low temperature assumption, one recovers the leading intrabranched contribution to $1/T_1$.

B. T_1^{-1} With Z_2 Symmetry, Subcritical Magnetic Field Results

Recall that for temperatures much smaller than the lowest gap, we need only consider the uniform part of the spin, \vec{l} . We are thus led to calculate the transition matrix between two single particle states

$$\vec{l}_{a,b}(k, k') \equiv \int_{-\infty}^{\infty} \frac{dq}{2\pi} \langle k, a | \vec{l}_q(t=0) | k', b \rangle \quad (3.21)$$

where $|k, a \rangle$ and $|k', b \rangle$ are magnon states, and a and b denote the different magnon branches.

The details of the calculation for the free fermion/boson models are given in the appendices.

Again, we perform this calculation in the low temperature limit ($\beta\omega_- \gg 1$). In this regime, and with an *anisotropic* hyperfine tensor, we expect the dominant transitions to be intrabranched unless the branches cross or come close to doing so (this in fact happens when the field is placed parallel to the low branch axis). We start by calculating intrabranched contributions in both boson and fermion models. The relevant component of \vec{l}_{--} is along the magnetic field. Taking this to be the 3 direction and the 1 direction corresponding to the RF field, Eq. (3.7) becomes

$$T_{1--}^{-1} \propto |A^{13}|^2 \frac{4}{(2\pi)} \int_0^\infty \frac{\omega_-(k) dk}{\sqrt{k^2 + \epsilon(k)^2}} e^{-\beta\omega_-(k)} \left(|l_{-,-}^3(k, k)|^2 + |l_{-,-}^3(-k, k)|^2 \right) \left(\frac{\partial\omega_-^2}{\partial k^2} \right)^{-1} \quad (3.22)$$

The function $\epsilon(k)$ is defined by

$$\omega_-(k^2 + \epsilon(k)^2) = \omega_N + \omega_-(k^2) \quad (3.23)$$

$$\epsilon(k)^2 \simeq \omega_N(2\omega_-(k^2) + \omega_N) \left(\frac{\partial\omega_-^2}{\partial k^2} \right)_{k=0}^{-1} \quad (3.24)$$

and the three branches have the following dispersion relations

$$\omega_\pm^2 = h^2 + v^2k^2 + \frac{(\Delta_1^2 + \Delta_2^2)}{2} \pm \sqrt{4h^2 \left(v^2k^2 + \frac{(\Delta_1^2 + \Delta_2^2)}{2} \right) + \frac{(\Delta_1^2 - \Delta_2^2)^2}{4}} \quad (3.25)$$

$$\omega_3^2 = v^2k^2 + \Delta_3^2 \quad \text{Bosons}$$

$$\omega_\pm^2 = h^2 + v^2k^2 + \frac{(\Delta_1^2 + \Delta_2^2)}{2} \pm \sqrt{4h^2 \left(v^2k^2 + \frac{(\Delta_1 + \Delta_2)^2}{4} \right) + \frac{(\Delta_1^2 - \Delta_2^2)^2}{4}} \quad (3.26)$$

$$\omega_3^2 = v^2k^2 + \Delta_3^2 \quad \text{Fermions}$$

When $\beta\omega_- \gg 1$ the integral in Eq. (3.22) is strongly peaked at $k = 0$. We can then make the following approximation (the validity of this will be discussed in a larger context later in this section):

$$T_{1--}^{-1} \propto 8|A^{13}|^2 C e^{-\beta\omega_-(0)} |l_{-,-}^3(0, 0)|^2 \frac{\omega_-(0)}{2\pi} \left(\frac{\partial\omega_-^2}{\partial k^2}(0) \right)^{-1} \quad (3.27)$$

$$C = \int_0^\infty dk \frac{e^{\beta(\omega_-(0) - \omega_-(k))}}{\sqrt{k^2 + \epsilon(k)^2}} \quad (3.28)$$

$$\approx \int_0^\infty dk \frac{e^{-\beta \left(\frac{\partial \omega_-^2}{\partial k^2} \right) \frac{k^2}{2\omega_-(0)}}}{\sqrt{k^2 + \epsilon(k)^2}}$$

Using Eq. (3.24) and making the change of variables $\beta \left(\frac{\partial \omega_-^2}{\partial k^2} \right) \frac{k^2}{2\omega_-(0)} \rightarrow k$, we get

$$\begin{aligned} C &= \int_0^\infty dk \frac{e^{-k^2}}{\sqrt{k^2 + \omega_N(2\omega_-(0) + \omega_N)\beta/2\omega_-(0)}} \\ &= e^{\omega_N(2\omega_-(0) + \omega_N)\beta/4\omega_-(0)} K_0(\omega_N(2\omega_-(0) + \omega_N)\beta/4\omega_-(0)) \end{aligned} \quad (3.29)$$

where K_0 is the zero order modified Bessel Function. For $\omega_-(0) \gg \omega_N$, which is really the case we are considering, this reduces to

$$C = -\log(\beta\omega_N/4) - \gamma. \quad (3.30)$$

This is identical to the factor arising in Eq. (3.9).

For the boson model (see Appendix A),

$$|l_{-,-}^3(0,0)|^2 = \frac{h^2}{\omega_-^2} \left(\frac{(\Delta_1^2 + \Delta_2^2) - \sqrt{2h^2(\Delta_1^2 + \Delta_2^2) + (\Delta_1^2 - \Delta_2^2)^2/4}}{\sqrt{2h^2(\Delta_1^2 + \Delta_2^2) + (\Delta_1^2 - \Delta_2^2)^2/4}} \right)^2 \quad (3.31)$$

so $F(h, T)$ goes to zero as a quadratic power of the field.

$$|l_{-,-}^3(0,0)|^2 \xrightarrow{h \rightarrow 0} \frac{h^2}{\Delta_2^2} \left(\frac{\Delta_1^2 + 3\Delta_2^2}{\Delta_1^2 - \Delta_2^2} \right)^2 \quad (3.32)$$

Where we assumed without loss of generality, $\Delta_2 < \Delta_1$. For the fermion model,

$$|l_{-,-}^3(0,0)|^2 = \frac{4h^2}{(\Delta_1 - \Delta_2)^2 + 4h^2} \quad (3.33)$$

This also vanishes with h^2 .

$$|l_{-,-}^3(0,0)|^2 \xrightarrow{h \rightarrow 0} \frac{4h^2\Delta_2^2}{(\Delta_1 - \Delta_2)^2} \quad (3.34)$$

We can also extend the above approximations to intrabranched transitions along the “+” branch and interbranch processes. The former amounts to letting $- \rightarrow +$:

$$T_{1++}^{-1} \propto 8|A^{13}|^2 e^{-\beta\omega_+(0)} |l_{+,+}^3(0,0)|^2 \frac{\omega_+(0)}{2\pi} \left(\frac{\partial \omega_+^2}{\partial k^2}(0) \right)^{-1} (-\log(\beta\omega_N/4) - \gamma) \quad (3.35)$$

The analogous expression for the interbranch rate is slightly more involved. Assuming that the branch labeled by r lies higher than that labeled by s , we can use the same approximations to arrive at

$$T_{1rs}^{-1} \propto 8e^{-\beta\omega_r(0)} \sum_i |A^{1i}|^2 \left[|l_{r,s}^i(0, Q)|^2 + |l_{r,s}^i(0, -Q)|^2 \right] \frac{\omega_r(0)}{2\pi} \left(\frac{\partial\omega_s^2}{\partial k^2}(Q) \right)^{-1/2} \left(\frac{\partial\omega_r^2}{\partial k^2}(0) \right)^{-1/2} \\ e^{\frac{Q^2 \left(\frac{\partial\omega_s^2}{\partial k^2}(Q) \right)}{4\omega_r(0)T}} K_0 \left(\frac{Q^2 \left(\frac{\partial\omega_s^2}{\partial k^2}(Q) \right)}{4\omega_r(0)T} \right) \quad (3.36)$$

Q is defined by $\omega_r(0) = \omega_s(Q)$. Notice that since S^3 is no longer a conserved operator, hence interbranch transitions $+ \leftrightarrow -$ are allowed.

Once more we define

$$T_1^{-1} = \sum_{ab} T_{1ab}^{-1} \equiv F(h, T) e^{-\beta\omega_-(0)} \quad (3.37)$$

where one is careful not to double count in summing over a and b .

There are regimes where it is no longer sufficient to calculate only one-particle transitions. When the temperature becomes comparable to the gap, multiparticle transitions become important. To include multiparticle transitions we simply replace the Boltzmann factor by appropriate occupation factors: $f_b(1 + f_b) = \text{cosech}^2(\frac{\beta\omega}{2})/4$ for bosons, and $f_f(1 - f_f) = \text{sech}^2(\frac{\beta\omega}{2})/4$ for fermions.¹⁵ At these temperatures it is also necessary to include the k -dependence of the integrand past the peak at the origin. We expect that at temperatures $T \approx \frac{\Delta}{3}$ and fields $h \approx \frac{2\Delta}{3}$ the numerically integrated results would differ from Eqns. (3.27–3.36) by about 10 percent. Since we have not yet obtained exact expressions for the contribution of the staggered part of the spin to the relaxation rate and since, in the regime in question, single magnon contributions are expected to compete with those from the uniform part of the spin (this will be demonstrated in the next section), we will not bother to present numerically integrated results in this paper.

In Figures 3–6 we use Eqns. (3.27, 3.35 and 3.36) to plot $F(h, T)$ for bosons and fermions and for fields along the crystal a, b and c directions in NENP. We use $\Delta_b = 2.52\text{mev}$, $\Delta_a = 1.17\text{mev}$ and $\Delta_c = 1.34\text{mev}$, and assume a uniform hyperfine coupling to all spin components on a given site. We do this for varying temperatures and try to consistently account for contributions from relevant transitions including interbranch and multiparticle effects. Within approximations used, multiparticle effects amount to multiplying the final expressions by $(1 \pm e^{-\beta\omega_s})^{-2}$.

$F(h, T)$ is shown for fields up to 9 Tesla even though the $(\beta\omega_- \gg 1)$ approximation is no longer valid at such fields. This is done to contrast the predictions of the boson and fermion models. It's easy to see that the boson result for $F(h, T)$ diverges at the critical field, while no such catastrophe is present in the fermion result. This divergence is logarithmic and infrared. It will persist even after account is made for the staggered part of the correlation function. Multiparticle scattering will in fact worsen the effect.

In NENP, when the field is along the b direction, we expect relevant interbranch transitions only for small field. In this regime, one must also be careful to include intrabranh transitions in the second lowest branch. All these processes are of the same order. Even though the intrabranh rates vanish at low fields, the interbranch contributions are suppressed by the absence of low momentum transitions (ie. Q for the interbranch transitions is $O(\sqrt{\Delta_1^2 - \Delta_2^2})$ as opposed to $O(\omega_N)$.) For this case, only l^3 need be calculated.

When the field is along the c direction (corresponding to the middle gap), we restrict ourselves to calculating intrabranh transitions along the lower branch and interbranch ones

between the lower and c branch. There are no intrabranh processes along the c axis. Calculating the interbranch transitions amounts to calculating $|l_{a,c}^1|^2$ and $|l_{a,c}^2|^2$.

When the field is along the a direction, the calculation proceeds as above. The crossing of the branches provides for an interesting effect. At the subcritical field where branch crossing occurs there is an infrared divergence in the density of states (ie. $\epsilon(k) \propto k$ for small k). We expect this to be suppressed by the finite width of the applied uniform field or by a cutoff corresponding to interchain coupling but a peak should be seen in T_1^{-1} at this point. This peak can also be used to locate the true ac -axes for the chain (however, effects discussed in the appendices may broaden this peak considerably).

As a brief aside, we would like to note that there are some curious differences in the behaviour of the boson matrix elements vs. that of the fermions. We have already seen that some transitions are fundamentally different in the two models even at low or zero fields. These may suggest experiments to further explore the nature of the low energy excitations in anisotropic Haldane gap materials. Even in the simple case of intrabranh backscattering the two theories differ (the fermion theory predicts a smaller, momentum dependent result). As another example, consider

$$\langle 0, -|S_{q=0}^i|0, 3 \rangle \quad (3.38)$$

ie. zero momentum transitions between the low branch and that parallel to the field (such a matrix element may be relevant in calculating ESR transition rates). The fermion model predicts a nearly field and gap independent result for such a rate in the limit $h \rightarrow 0$. The boson model prediction, however, is strongly dependent on the ratio of the gaps and therefore on the orientation of the field. To some degree, the reason that the theories feature such differences *even in the isotropic case*, is that the generator of rotational symmetry is fundamentally different in the two theories: the fermion magnetization does not couple left and right moving fermions, while the boson operator does. In particular, this means that intrabranh backscattering should vanish with the fermion mass, while no such miracle occurs with the bosons.

There are some puzzling discrepancies between our result for $F(h, T)$ and that of Ref. (9). At about 5 Tesla, the experimental data gives $F_b < F_c$ while our theoretical calculation gives the reverse at low temperatures. Moreover, the ‘flatter’ of the experimental curves is the one corresponding to the field perpendicular to the chain axis (about which there is approximate $U(1)$ symmetry). The behaviour of the theories is quite easy to understand from the universal results valid in the axially symmetric case, discussed in Section (III.A). F_b is roughly independent of field with axial symmetry since l_{--}^3 is nearly h independent (in fact, F_b exhibits a logarithmic divergence as $h \rightarrow 0$). On the other hand, F_c vanishes quadratically as $h \rightarrow 0$. Including the small breaking of the axial symmetry corresponding to $\Delta_c - \Delta_a = 2^\circ K$, F_b is essentially constant down to low fields of order $\Delta_c - \Delta_a \approx 1T$, before rapidly decreasing as seen in the figures. Given the original Hamiltonian, Eq. (1.1), we expect that our calculations are at least qualitatively correct.

Finally, we would like to mention some recent NMR data collected on the 1-D $S = 1$ spin chain $AgVP_2S_6$ by Takigawa et. al.¹⁶. This material is highly one dimensional with a large gap ($\Delta \sim 320^\circ K$) and very nearly isotropic ($\delta \sim 4^\circ K$). These characteristics make it ideal for analysis using our results. There are, however, some questions about the

properties of the material which would have to be analyzed before an understanding of the NMR results is possible within the framework proposed here. The gap deduced from studies on the Vanadium atom ($\Delta \sim 410^\circ K$) conflicts significantly with those performed on the Phosphorous sites and with neutron scattering data. In addition, the material has very low symmetry (corresponding to the space group $P2/a$) and very little is known about the possible small E and D terms in the Hamiltonian and their corresponding symmetry. There is fair qualitative agreement between the ^{31}P NMR data and our theory, and it is possible to explain some of the discrepancies using a temperature dependent anisotropic gap structure, but we feel that not enough is yet understood about gross features of the material to justify such speculation at this time.

IV. CLOSE TO THE CRITICAL FIELD

In this final section we would like to demonstrate that the staggered correlator contribution becomes crucial as $h \rightarrow h_c$ from below. First, we would like to describe the transition rate due to the uniform part of the spin-spin correlation close to the critical field, $h_c - h \ll k_b T$. In this limit, the long wavelength modes dominate the physics, and only intrabranch processes need be considered. Since the fermion model becomes exact in this limit, we will rely on its predictions. In the Z_2 case, the dispersion relation becomes

$$\omega(k, h) = \sqrt{v_e^2 k^2 + \Delta_e^2} \quad (4.1)$$

where $v_e^2 = v^2 \frac{(\Delta_1 - \Delta_2)^2}{(\Delta_1 + \Delta_2)^2}$ and the gap is $\Delta_e^2 = (h - h_c)^2 \Delta_1 \Delta_2 / (\Delta_1 + \Delta_2)^2$.

The $U(1)$ case is different: the dispersion relation in the long wavelength limit is

$$\omega(k, h) = |(h_c - h) + \frac{v^2 k^2}{2h_c}| \quad (4.2)$$

In the fermion model, the coupling of the magnetic field to a *conserved* charge serves as a chemical potential for the magnon states. At criticality the dispersion is quadratic as opposed to linear as in the Z_2 case. Above h_c the chemical potential drops below zero indicating that the ground state is now magnetic and filled with quasiparticles.

In calculating the uniform spin contribution we must now include the appropriate occupation numbers in Eq. (3.22):

$$(T_1^{-1})_{\text{Unif}} \propto \frac{4|A^{13}|^2}{2\pi} \int_0^\infty dk \frac{\omega f_f(\omega)(1 - f_f(\omega))}{\sqrt{k^2 + \epsilon(k)^2}} \left(\frac{\partial \omega^2}{\partial k^2} \right)^{-1} (|l_{-,-}^3(k, k)|^2 + |l_{-,-}^3(k, -k)|^2) \quad (4.3)$$

In the $U(1)$ case we get a similar equation to (3.8) but with appropriate occupation factors. The behaviour is logarithmic with temperature at $T \gg \omega_N$ even at the critical point.

In the Z_2 case we get

$$(T_1^{-1})_{\text{Unif}} \approx \frac{2|A^{13}|^2}{\pi v^2} \frac{\Delta_1 \Delta_2}{(\Delta_1 - \Delta_2)^2} \int_0^\infty dk \frac{(\omega + \omega_N) \operatorname{cosech}^2(\frac{\beta\omega}{2})}{\sqrt{(\omega + \omega_N)^2 - \Delta_e^2}} \quad (4.4)$$

At criticality, we set $\omega \propto k$ and $\Delta_e = 0$. We may simply rescale the integration variable to obtain

$$(1/T_1)_{\text{Unif}} \propto T \quad (4.5)$$

in the limit that $\omega_N \ll T$. This is expected from the Ising model where the uniform part of the spin corresponds to the Ising energy density operator, ϵ , of scaling dimension 1. In terms of Majorana fermions this operator is $\psi_L \psi_R = \epsilon$.

We can also say something about the behaviour of the staggered part of the correlation function at criticality. In both $U(1)$ and Ising cases we know the critical behaviours of the staggered spin correlators. In both cases, the magnetic field acts as the temperature (and the temperature acts as the Euclidean time interval in an analogous 2D classical system). On the infinite Euclidean plane these correlators are⁴:

$$\langle \phi^\dagger(z)\phi(0) \rangle \sim 1/|z|^{\frac{1}{2}} \quad (4.6)$$

$$\langle \sigma(z)\sigma(0) \rangle = 1/|z|^{\frac{1}{4}} \quad (4.7)$$

The field $\phi = \phi^x + i\phi^y$ is the charged $U(1)$ field of the boson model; σ is the disorder field of the Ising model (highly non-local in fermionic language) – it is the only local non-trivial primary operator aside from the energy density ϵ . To get the finite temperature result, we simply make the conformal transformation from the plane into the finite strip¹⁷, $z_p = e^{2\pi iz_s/\beta}$ to get

$$\begin{aligned} \langle \sigma(z)\sigma(0) \rangle &= \frac{(\pi/\beta)^{\frac{1}{4}}}{|\sin(\pi z/\beta)|^{\frac{1}{4}}} \\ \langle \phi^\dagger(z)\phi(0) \rangle &= \frac{(\pi/\beta)^{\frac{1}{2}}}{|\sin(\pi z/\beta)|^{\frac{1}{2}}} \end{aligned} \quad (4.8)$$

To get the contribution to T_1^{-1} we integrate over $\int dt e^{i\omega_N t}$ and set $z = it + \epsilon$.

$$(T_1^{-1})_{\text{Stag}} \propto \int_{-\infty}^{\infty} dt \frac{e^{i\omega_N t}}{\beta^{\frac{1}{x}} |\sin(\pi z/\beta)|^{\frac{1}{x}}} \quad (4.9)$$

x is either 4 or 2.

Since this is analytic as $\omega_N \rightarrow 0$, we get that in the experimentally important limit $T \gg \omega_N$

$$\begin{aligned} (T_1^{-1})_{\text{Stag}} &\propto T^{-3/4} + O(\omega_N) && \text{Ising case} \\ (T_1^{-1})_{\text{Stag}} &\propto T^{-1/2} + O(\omega_N) && U(1) \text{ case} \end{aligned} \quad (4.10)$$

In the low T limit, this will be significantly stronger than the contribution from the uniform part of the correlator in both theories. In fact, as long as we are sufficiently close to the critical regime the above results will only be suppressed by factors of order $O(\Delta/T)$, where Δ is the gap and $\Delta \ll T$. Thus in this regime, even slightly away from criticality, we

see that the most important contribution to $1/T_1$ comes from $q = \pi$, ie. the staggered part of the spin correlation function.

Farther still from criticality, the analysis breaks down but we expect the staggered spin contribution to influence $1/T_1$ through the region $T = O(\Delta(h))$.

Acknowledgements

We thank WJL Buyers and E. Sørensen for helpful discussions. J.S. would like to thank M. Walker and his research group at the University of Toronto where some of this work was done. This research was supported in part by NSERC.

APPENDIX A: DIAGONALIZING THE BOSON/FERMIONS MODELS

To do the necessary calculations we need to have a basis of eigenstates for the Hamiltonian and know the expansion of the field operators in terms of creation/annihilation operators for these states. Obtaining this is tedious (especially when the field does not lie in a direction of symmetry, for then all the branches mix) but the idea is to find the right Bogoliubov transformation which diagonalizes H . We do this first for the Boson model.

As discussed in [18], we seek to find the eigenvectors of the (non-hermitian) matrix ηM , where

$$H_k = \vec{a}_k^\dagger \mathbf{A} \vec{a}_k + \vec{a}_{-k}^\dagger \mathbf{A}^* \vec{a}_{-k} + \vec{a}_k^\dagger \mathbf{B} \vec{a}_{-k}^\dagger + \vec{a}_k \mathbf{B}^* \vec{a}_{-k} \quad (\text{A1})$$

$$\eta M = \begin{pmatrix} \mathbf{A} & \mathbf{B} \\ -\mathbf{B}^* & -\mathbf{A}^* \end{pmatrix} \quad (\text{A2})$$

We will now find the eigenvectors in the case where the field lies in a direction of symmetry. In this case, only the excitations transverse to the direction of the applied field mix and we need only solve a (4×4) set of equations. Considering the two mixed components of $\vec{\phi}$, we write

$$\phi^i(k, t=0) = \frac{1}{\sqrt{2\omega_0}} [a_{-k}^{i\dagger} + a_k^i] \quad (\text{A3})$$

$$\pi^i(k, t=0) = i\sqrt{\frac{\omega_0}{2}} [a_{-k}^{i\dagger} - a_k^i] \quad (\text{A4})$$

$$[a_k^i, a_{k'}^{j\dagger}] = 2\pi\delta_{ij}\delta(k - k') \quad (\text{A5})$$

ω_0 is arbitrary.

Plugging this into the Hamiltonian, we then have that

$$\mathbf{A} = \frac{\omega_0}{4}\mathbf{I} + \frac{\mathbf{K}}{4\omega_0} - \frac{1}{2}h\sigma_2 \quad (\text{A6})$$

$$\mathbf{B} = -\frac{\omega_0}{4}\mathbf{I} + \frac{\mathbf{K}}{4\omega_0} \quad (\text{A7})$$

where σ_2 is the usual Pauli matrix, and

$$\mathbf{K} = \text{diag}(\Delta_1^2 + v^2k^2, \Delta_2^2 + v^2k^2) \quad (\text{A8})$$

Summarizing the above, we need to solve:

$$0 = \begin{pmatrix} \frac{\omega_0}{4}\mathbf{I} + \frac{\mathbf{K}}{4\omega_0} - \frac{1}{2}h\sigma_2 - \frac{\omega}{2}\mathbf{I} & -\frac{\omega_0}{4}\mathbf{I} + \frac{\mathbf{K}}{4\omega_0} \\ \frac{\omega_0}{4}\mathbf{I} - \frac{\mathbf{K}}{4\omega_0} & -\frac{\omega_0}{4}\mathbf{I} - \frac{\mathbf{K}}{4\omega_0} - \frac{1}{2}h\sigma_2 - \frac{\omega}{2}\mathbf{I} \end{pmatrix} \quad (\text{A9})$$

which can be manipulated to give

$$0 = \begin{pmatrix} (\omega_0 - \omega)\mathbf{I} - h\sigma_2 & -(\omega_0 + \omega)\mathbf{I} - h\sigma_2 \\ \frac{\mathbf{K}}{\omega_0} - \omega\mathbf{I} - h\sigma_2 & \frac{\mathbf{K}}{\omega_0} + \omega\mathbf{I} + h\sigma_2 \end{pmatrix} \quad (\text{A10})$$

The eigenvalues of ηM are already known, as they are the solutions to the classical equations of motion and come in pairs $\pm\omega_{\pm}$ (see eqn. 3.25). Furthermore, we need only work to find one eigenvector of each pair because if $\begin{pmatrix} X \\ Y \end{pmatrix}$ is a right-eigenvector of ηM with eigenvalue ω , then $\begin{pmatrix} Y^* \\ X^* \end{pmatrix}$ is a right-eigenvector of ηM with eigenvalue $-\omega$ (X and Y are themselves two-component vectors).

The bottom rows give the following set of equations

$$0 = (\Delta_1^2 + v^2k^2)\chi_{\pm,1} - \omega_0\omega_{\pm}\xi_{\pm,1} + ih\omega_0\xi_{\pm,2} \quad (\text{A11})$$

$$0 = (\Delta_2^2 + v^2k^2)\chi_{\pm,2} - \omega_0\omega_{\pm}\xi_{\pm,2} - ih\omega_0\xi_{\pm,1} \quad (\text{A12})$$

where it turns out to be convenient to work with $\chi \equiv X + Y$ and $\xi \equiv X - Y$. The top rows can be manipulated to give

$$0 = (h^2 - \omega_{\pm}^2)\chi_{\pm,2} - ih\omega_0\xi_{\pm,1} + \omega_0\omega_{\pm}\xi_{\pm,2} \quad (\text{A13})$$

$$0 = -(h^2 - \omega_{\pm}^2)\chi_{\pm,1} - ih\omega_0\xi_{\pm,2} - \omega_0\omega_{\pm}\xi_{\pm,1} \quad (\text{A14})$$

These can then be worked to give

$$(\Delta_1^2 + v^2k^2 + \omega_{\pm}^2 - h^2)\chi_{\pm,1} = 2\omega_0\omega_{\pm}\xi_{\pm,1} \quad (\text{A15})$$

$$(\Delta_2^2 + v^2k^2 + \omega_{\pm}^2 - h^2)\chi_{\pm,2} = 2\omega_0\omega_{\pm}\xi_{\pm,2} \quad (\text{A16})$$

$$(h^2 + \Delta_1^2 + v^2k^2 - \omega_{\pm}^2)\chi_{\pm,1} = -2ih\omega_0\xi_{\pm,2} \quad (\text{A17})$$

$$(h^2 + \Delta_2^2 + v^2k^2 - \omega_\pm^2)\chi_{\pm,2} = 2ih\omega_0\xi_{\pm,1} \quad (\text{A18})$$

Note that if we fix the phase of X_1 to be real then Y_1 must also be real as X_2 and Y_2 must be pure imaginary. The normalization condition now allows us to solve for the eigenvectors which form the columns of the transformation matrix between the old and diagonal basis of creation/annihilation operators. This normalization condition is slightly unusual since ηM is not hermitean: $X^\dagger X - Y^\dagger Y = 1$. In terms of χ and ξ this is

$$\chi_{\pm,1}\xi_{\pm,1} - \chi_{\pm,2}\xi_{\pm,2} = 1 \quad (\text{A19})$$

The solution is

$$\chi_{\pm,1} = \left(\frac{\omega_0\omega_\pm(h^2 + \Delta_2^2 + v^2k^2 - \omega_\pm^2)}{(\Delta_1^2 + v^2k^2 + \omega_\pm^2 - h^2)(h^2 + \frac{\Delta_1^2 + \Delta_2^2}{2} + v^2k^2 - \omega_\pm^2)} \right)^{1/2} \quad (\text{A20})$$

$$\xi_{\pm,1} = \frac{\Delta_1^2 + v^2k^2 + \omega_\pm^2 - h^2}{2\omega_0\omega_\pm} \chi_{\pm,1} \quad (\text{A21})$$

$$\chi_{\pm,2} = \frac{2ih\omega_0}{h^2 + \Delta_2^2 + v^2k^2 - \omega_\pm^2} \xi_{\pm,1} \quad (\text{A22})$$

$$\xi_{\pm,2} = \frac{\Delta_2^2 + v^2k^2 + \omega_\pm^2 - h^2}{2\omega_0\omega_\pm} \chi_{\pm,2} \quad (\text{A23})$$

We can define the matrices χ and ξ with the rows labeled by the eigenvalues (+, -) and the columns labeled by the original masses (1, 2). One easily verifies that in the limit $h \rightarrow 0$ these become

$$\chi = \xi^{-1\dagger} = \begin{pmatrix} \sqrt{\frac{\omega_0}{\sqrt{\Delta_1^2 + v^2k^2}}} & 0 \\ 0 & i\sqrt{\frac{\omega_0}{\sqrt{\Delta_2^2 + v^2k^2}}} \end{pmatrix} \quad (\text{A24})$$

While in the limit $\Delta_2 \rightarrow \Delta_1$,

$$\chi = \frac{\omega_0}{\sqrt{\Delta^2 + v^2k^2}} \xi = \sqrt{\frac{\omega_0}{2\sqrt{\Delta^2 + v^2k^2}}} \begin{pmatrix} 1 & -i \\ 1 & i \end{pmatrix} \quad (\text{A25})$$

It turns out that

$$\vec{\phi}(k, t = 0) = \frac{1}{\sqrt{2\omega_0}} [\chi^\dagger \vec{b}_{-k}^\dagger + \chi^T \vec{b}_k] \quad (\text{A26})$$

$$\vec{\pi}(k, t = 0) = i\sqrt{\frac{\omega_0}{2}} [\xi^\dagger \vec{b}_{-k}^\dagger - \xi^T \vec{b}_k] \quad (\text{A27})$$

Where the b 's are the operators which diagonalize H .

So now we have all the equipment necessary to calculate $\vec{l}_{a,b}(k, k')$.

$$\vec{l}_{a,b}(k, k') = \frac{-i}{2} \left(\xi^*(k) \vec{\Sigma} \chi^T(k') + \chi^*(k) \vec{\Sigma} \xi^T(k') \right)_{a,b} \quad (\text{A28})$$

where we define the cross product matrix with the Levi-Civita symbol by $\Sigma^i = \epsilon^{ijk}$. The matrices, χ and ξ , are now three by three with the inclusion of the trivially diagonal unmixed component (ie. the three component): $\chi_{33} = \sqrt{\frac{\omega_0}{\sqrt{\Delta_3^2 + v^2 k^2}}}$ and $\xi_{33} = \sqrt{\frac{\sqrt{\Delta_3^2 + v^2 k^2}}{\omega_0}}$.

We would now like to repeat this diagonalization procedure for the Fermion model. The free Hamiltonian is

$$\mathcal{H}(x) = \frac{1}{2} \left[\vec{\psi}_L \cdot iv \partial_x \vec{\psi}_L - \vec{\psi}_R \cdot iv \partial_x \vec{\psi}_R + i \sum_{i=1}^3 \Delta_i (\psi_{R,i} \psi_{L,i} - \psi_{L,i} \psi_{R,i}) + i \vec{h} \cdot (\vec{\psi}_L \times \vec{\psi}_L + \vec{\psi}_R \times \vec{\psi}_R) \right] \quad (\text{A29})$$

Setting $v = 1$, we can write

$$\vec{\psi}_R = \int_0^\infty \frac{dk}{2\pi} \left(e^{-ik(t-x)} \vec{a}_{R,k} + e^{ik(t-x)} \vec{a}_{R,k}^\dagger \right) \quad (\text{A30})$$

$$\vec{\psi}_L = \int_0^\infty \frac{dk}{2\pi} \left(e^{-ik(t+x)} \vec{a}_{L,k} + e^{ik(t+x)} \vec{a}_{L,k}^\dagger \right) \quad (\text{A31})$$

$$\{a_k^i, a_{k'}^j\} = 2\pi \delta_{ij} \delta(k - k') \quad (\text{A32})$$

the Hamiltonian density in k -space becomes

$$H_k = \vec{\alpha}_k^\dagger M_k \vec{\alpha}_k \quad (\text{A33})$$

where

$$M = \begin{pmatrix} \mathbf{Ik} - i\vec{h} \times & i\Delta \\ -i\Delta & -\mathbf{Ik} - i\vec{h} \times \end{pmatrix} \quad (\text{A34})$$

$$\vec{\alpha}_k = \begin{pmatrix} \vec{a}_{R,k} \\ \vec{a}_{L,k}^\dagger \end{pmatrix} \quad (\text{A35})$$

The idea now is to diagonalize this matrix and find the eigenvalues and eigenvectors. In other words, find the unitary transformation which diagonalizes H . We assume the field is in a direction of symmetry so that we need only diagonalize a 4×4 matrix. Given that the field is in the 3 direction, the eigenvalues for the mixed states are $\pm \omega_\pm$ from eqn. 3.26. It may be more illuminating to write out M in a basis that is more natural to the $U(1)$ problem. Using

$$\begin{pmatrix} a_{R,k}^1 \\ a_{R,k}^2 \end{pmatrix} = \frac{1}{\sqrt{2}} \begin{pmatrix} 1 & 1 \\ i & -i \end{pmatrix} \begin{pmatrix} a_{R,k}^+ \\ a_{R,k}^- \end{pmatrix} \quad (\text{A36})$$

$$\begin{pmatrix} a_{L,k}^{1\dagger} \\ a_{L,k}^{2\dagger} \end{pmatrix} = \frac{1}{\sqrt{2}} \begin{pmatrix} 1 & 1 \\ -i & i \end{pmatrix} \begin{pmatrix} a_{L,k}^{+\dagger} \\ a_{L,k}^{-\dagger} \end{pmatrix} \quad (\text{A37})$$

In this basis, M becomes

$$M = \begin{pmatrix} k\mathbf{I} - \mathbf{h}\sigma_3 & i\Delta\sigma_1 + i\delta\mathbf{I} \\ -i\Delta\sigma_1 - i\delta\mathbf{I} & -k\mathbf{I} + \mathbf{h}\sigma_3 \end{pmatrix} \quad (\text{A38})$$

Where $\Delta = \frac{\Delta_1 + \Delta_2}{2}$ and $\delta = \frac{\Delta_1 - \Delta_2}{2}$. The equations for the components of the eigenvectors possess the symmetries

$$u_1 \leftrightarrow u_2, u_3 \leftrightarrow u_4, h \leftrightarrow -h \quad (\text{A39})$$

$$u_1 \leftrightarrow u_3, u_2 \leftrightarrow u_4, \omega \leftrightarrow -\omega \quad (\text{A40})$$

where ω is the eigenvalue. After some algebra,

$$u_4 = \frac{2i\Delta(k - \omega)}{\omega^2 + \Delta^2 - (k + h)^2 - \delta^2} u_1 \quad (\text{A41})$$

$$u_3 = \frac{2i\delta(k - \omega)}{(\omega - h)^2 - k^2 + \delta^2 - \Delta^2} u_1 \quad (\text{A42})$$

$$u_2 = \frac{2i\Delta(k + \omega)}{\omega^2 + \Delta^2 - (k + h)^2 - \delta^2} u_3 \quad (\text{A43})$$

Using the normalization condition,

$$\sum_{i=1}^4 |u_i|^2 = 1 \quad (\text{A44})$$

we set the phase of u_1 to be real for positive eigenvalues; the above symmetries allow us the freedom to choose a convenient phase for u_1 corresponding to negative eigenvalues.

$$u_1 = 2\delta(k + \omega)(\omega^2 + \Delta^2 - (k + h)^2 - \delta^2) \div [4\delta^2(k + \omega)^2((\omega^2 + \Delta^2 - (k + h)^2 - \delta^2)^2 + 4\Delta^2(k - \omega)^2) + ((\omega + h)^2 - k^2 + \delta^2 - \Delta^2)^2((\omega^2 + \Delta^2 - (k + h)^2 - \delta^2)^2 + 4\Delta^2(k + \omega)^2)]^{\frac{1}{2}} \quad (\text{A45})$$

We define the 6×6 diagonalizing matrix with columns given by the eigenvectors \vec{u}_ω as

$$X_{i,\omega} = (u_{\omega_+}^i, u_{\omega_-}^i, u_{\omega_3}^i, u_{-\omega_+}^i, u_{-\omega_-}^i, u_{-\omega_3}^i) \quad (\text{A46})$$

$$\alpha_k^i = UX_\omega^i \beta^\omega \quad (\text{A47})$$

$$U = \frac{1}{\sqrt{2}} \begin{pmatrix} 1 & 1 & 0 & 0 & 0 & 0 \\ i & -i & 0 & 0 & 0 & 0 \\ 0 & 0 & \sqrt{2} & 0 & 0 & 0 \\ 0 & 0 & 0 & 1 & 1 & 0 \\ 0 & 0 & 0 & -i & i & 0 \\ 0 & 0 & 0 & 0 & 0 & \sqrt{2} \end{pmatrix} \equiv \begin{pmatrix} V & 0 \\ 0 & V\sigma_1 \end{pmatrix} \quad (\text{A48})$$

The diagonal operators, β^ω are defined as:

$$\vec{\beta}_k = \begin{pmatrix} \vec{c}_k \\ \vec{d}_k^\dagger \end{pmatrix} \quad (\text{A49})$$

Our freedom in choosing the phases for the eigenvectors corresponding to negative eigenvalues allow us to write

$$X = \begin{pmatrix} R & T \\ T & R \end{pmatrix} \quad (\text{A50})$$

The d 's and c 's correspond to left and right moving fermions, respectively. This becomes clear in the limit $\Delta_1 \rightarrow \Delta_2 \rightarrow 0$.

Some limiting forms of R and T are:

$$R(h \rightarrow 0) = \frac{1}{2} \begin{pmatrix} \sqrt{\frac{\omega_1+k}{\omega_1}} & -\sqrt{\frac{\omega_2+k}{\omega_2}} & 0 \\ \sqrt{\frac{\omega_1+k}{\omega_1}} & \sqrt{\frac{\omega_2+k}{\omega_2}} & 0 \\ 0 & 0 & \sqrt{2\frac{\omega_3+k}{\omega_3}} \end{pmatrix} \quad (\text{A51})$$

$$T(h \rightarrow 0) = \frac{1}{2} \begin{pmatrix} -i\sqrt{\frac{\omega_1-k}{\omega_1}} & -i\sqrt{\frac{\omega_2-k}{\omega_2}} & 0 \\ -i\sqrt{\frac{\omega_1-k}{\omega_1}} & i\sqrt{\frac{\omega_2-k}{\omega_2}} & 0 \\ 0 & 0 & -i\sqrt{2\frac{\omega_3-k}{\omega_3}} \end{pmatrix} \quad (\text{A52})$$

$$R(\delta \rightarrow 0) = \frac{1}{\sqrt{2}} \begin{pmatrix} 0 & -\sqrt{\frac{\omega_\Delta+k}{\omega_\Delta}} & 0 \\ \sqrt{\frac{\omega_\Delta+k}{\omega_\Delta}} & 0 & 0 \\ 0 & 0 & \sqrt{\frac{\omega_3+k}{\omega_3}} \end{pmatrix} \quad (\text{A53})$$

$$T(\delta \rightarrow 0) = \frac{1}{\sqrt{2}} \begin{pmatrix} -i\sqrt{\frac{\omega_\Delta-k}{\omega_\Delta}} & 0 & 0 \\ 0 & i\sqrt{\frac{\omega_\Delta-k}{\omega_\Delta}} & 0 \\ 0 & 0 & -i\sqrt{\frac{\omega_3-k}{\omega_3}} \end{pmatrix} \quad (\text{A54})$$

The expression for the uniform part of the spin in terms of fermions is

$$\frac{-i}{2} (\vec{\psi}_L \times \vec{\psi}_L + \vec{\psi}_R \times \vec{\psi}_R) \quad (\text{A55})$$

We can write $\vec{l}_{a,b}(k, k')$ as

$$\vec{l}_{a,b}(k, k') = -i \int_0^\infty dp dq \langle k, a | (\vec{\alpha}_p^\dagger + \vec{\alpha}_p^T) \begin{pmatrix} \vec{\Sigma} & 0 \\ 0 & \vec{\Sigma} \end{pmatrix} (\vec{\alpha}_q + \vec{\alpha}_q^*) | k', b \rangle \quad (\text{A56})$$

where again Σ is the cross product matrix.

After some algebra, we get

$$\vec{l}_{a,b}(k, k') = -i \begin{pmatrix} R^\dagger V^\dagger \vec{\Sigma} V R + T^\dagger \sigma_1 V^\dagger \vec{\Sigma} V \sigma_1 T & R^\dagger V^\dagger \vec{\Sigma} V^* T^* + T^\dagger \sigma_1 V^\dagger \vec{\Sigma} V^* \sigma_1 R^* \\ T^T V^T \vec{\Sigma} V R + R^T \sigma_1 V^T \vec{\Sigma} V \sigma_1 T & T^T V^T \vec{\Sigma} V^* T^* + R^T \sigma_1 V^T \vec{\Sigma} V^* \sigma_1 R^* \end{pmatrix} \quad (\text{A57})$$

Each index of this matrix runs over six states; the first and last three correspond to right and left movers respectively. In the case of $U(1)$ symmetry each set would correspond to states of definite spin.

APPENDIX B: IMPURITY EFFECTS ON $1/T_1$

The NMR experiments done on NENP have exhibited curious behaviour at small fields (0-4 T) and low temperatures. In this regime, our calculations have shown that $1/T_1$ should decrease rapidly with decreasing applied field. Experiments, however, indicate a non-zero lifetime at $h = 0$ that undergoes a minimum at about 2 T before showing the expected exponential behaviour at around 4 T. Moreover, the zero field lifetime increases with temperature.⁹

If one attempted to fit the mid field data (which is expected to be in good agreement with our calculations) to our results and assumed that there is no other mechanism for relaxation, then the observed values would deviate from the calculated ones at low fields ($h = .2 - 3$ Tesla) by a factor as big as 300 for $T = 1.4$ Kelvin.

Clearly the low field bump is an impurity effect. Dynamics due to dimensional crossover are ruled out by the fact that $1/T_1$ increases with temperature at the low fields discussed. A possible, yet not fully convincing contribution can come from the dynamics of the spin- $\frac{1}{2}$ degrees of freedom at the ends of large but *finite* chains in NENP. This is discussed further in ref. [6]. The essential physics is that the resonance energy of a spin- $\frac{1}{2}$ at a chain end in a uniform field crossed with an RF field is broadened by the interaction with thermally excited magnons even at temperatures well below the gap. At the Larmor frequency of a Hydrogen nucleus and low magnetic field, the Fourier transform of the local spin-spin correlator (which is proportional to $1/T_1$) is of the form:⁶

$$1/T_{1_{Imp}} \propto e^{-\Delta/T} \quad (\text{B1})$$

This is true in both the limits of long and short chains. In both instances this is not consistent with the weaker temperature dependence seen at constant low magnetic field. We conclude that the experimental results are due to a mechanism not intrinsic to the Haldane system or coupled to it.

APPENDIX C: THE STRUCTURE OF NENP AND EXPERIMENTAL RAMIFICATIONS

Each chain in NENP is comprised of Ethylenediamine-Nickel chelates separated by nitrite groups. It is important to realize, however, that two neighbouring Ni^{2+} are not equivalent; rather, one is related to the other by a π rotation about the b axis. Also, the angle along the $N - Ni - O$ bond is not exactly π , meaning that the Ni site is not truly centrosymmetric. Most importantly, the local symmetry axes of each Ni ion are rotated with respect to the abc (crystallographic) axes. To demonstrate this we now note the coordinates of the Nitrogen atoms in the Ethylenediamine chelate surrounding the Nickel (placing the Nickel at the origin):¹⁹

Atom	a (Å)	b (Å)	c (Å)
$N(1)$	2.053 (3)	.162 (3)	.338 (3)
$N(2)$.619 (3)	-.184 (3)	-1.971 (3)

The other Nitrogen atoms in the chelate can be obtained by reflection through the Nickel. One easily sees that projecting this structure onto the b plane yields symmetry axes (in the b plane) rotated $\sim 60^\circ$ from the ac -axes. This is shown in Fig. 7. The inclination of the local Nickel axes from the abc system can be obtained by taking the cross product of the two Nitrogen vectors (ie. the normal to the plane described by the four Nitrogen atoms in the chelate):

$$\hat{n} = (-.06 (1), .98 (1), -.11 (1)) \tag{C1}$$

From the above, it is clear that the local Ni b' -axis makes a $\sim 10^\circ$ angle with the b -axis, while the azimuthal angle in the ac plane is $\sim -28^\circ$ from c . The 10° tilt is roughly about the a' direction of the local symmetry axes.

One may worry that the NO_2 radicals may distort the local symmetry axes, but remarkably enough, when projected onto the ac plane, the three atoms in the molecule sit on the c' axis. This reinforces our suspicion that the local symmetry axes are indeed what we have above.

Next, we consider the whole space group of NENP. The most recent attempt to solve for the crystal symmetries has concluded that the true space group of the material is $Pn2_1a$ ¹⁹; this is a non-centrosymmetric space group with a screw 2_1 symmetry about the b axis, diagonal glide plane reflection symmetry along the a axis, and an axial glide plane reflection symmetry along c . Experimentally, attempts to solve the structure in $Pn2_1a$ have not been successful; rather, it seems that $Pnma$ gives a better fit. The main difference between the two is the presence in $Pnma$ of a mirror plane parallel to b at $\frac{1}{4}b$, centers of symmetry at various locations in the unit cell, and two-fold screw axes separating these centers of symmetry. The reason for the experimental discrepancy is attributed to disorder in the orientation of the nitrite group, the perchlorate anions, and the existence of a local or pseudo center of symmetry lying very close to the Ni (thousandths of an Angstrom)¹⁹. A crucial point is that both space groups share the axial glide planes along a , the diagonal glide planes along

C and the 2_1 screw symmetry about b . These generate a total of 4 Ni sites per primitive cell and two chains through each cell. The two chains are such that the Ni chelates on one are the mirror image of the other. Figure 8 shows a projection of this picture onto the ac plane.

The presence of the 2_1 screw symmetry about each chain axis introduces staggered contributions to the local anisotropy and gyromagnetic tensors. This is because, as motivated above, these are not diagonal in the crystallographic coordinate system. The resulting spin Hamiltonian is

$$H = J \sum_i \left[\vec{S}_i \cdot \vec{S}_{i+1} + \vec{S}_i \cdot \mathbf{D} \vec{S}_i - \mu_B \vec{S}_i \cdot \mathbf{G} \vec{H} + (-1)^i (\vec{S}_i \cdot \mathbf{d} \vec{S}_i - \mu_B \vec{S}_i \cdot \mathbf{g} \vec{H}) \right] \quad (C2)$$

We make the assumption that the symmetry of the mass and g -tensors is the same (ie. that at each site they can be simultaneously diagonalized). We can get the required parametrization for the g -tensors from high temperature uniform susceptibility data¹⁹. This is based on the idea that at high temperatures the Ni atoms will behave as an ensemble of uncoupled spins ($s = 1$) with the same gyromagnetic tensor as in the antiferromagnetic case. With this in mind we get

$$\mathbf{G} = \begin{pmatrix} G_{c'} \cos^2(\theta) + G_{b'} \sin^2(\theta) & 0 & 0 \\ 0 & G_{a'} & 0 \\ 0 & 0 & G_{b'} \cos^2(\theta) + G_{c'} \sin^2(\theta) \end{pmatrix} \quad (C3)$$

$$\mathbf{g} = \begin{pmatrix} 0 & 0 \sin(\theta) \cos(\theta) (G_{b'} - G_{c'}) \\ 0 & 0 & 0 \\ \sin(\theta) \cos(\theta) (G_{b'} - G_{c'}) & 0 & 0 \end{pmatrix} \quad (C4)$$

Here $\theta \sim 10^\circ$, and $G_{a'} = 2.24$, $G_{b'} = 2.15$, $G_{c'} = 2.20$ are the values for the local G -tensor that give the observed high temperature g -tensor when averaged over the unit cell. Correspondingly, the mass tensors must have the following form:

$$\mathbf{D} = \begin{pmatrix} D_{c'} & 0 & 0 \\ 0 & D_{a'} & 0 \\ 0 & 0 & D_{b'} \end{pmatrix} \quad (C5)$$

$$\mathbf{d} = \begin{pmatrix} 0 & 0 & \frac{\tan(2\theta)}{2} (D_{b'} - D_{c'}) \\ 0 & 0 & 0 \\ \frac{\tan(2\theta)}{2} (D_{b'} - D_{c'}) & 0 & 0 \end{pmatrix} \quad (C6)$$

The parameters $D_{a'}$, $D_{c'}$, $D_{b'}$ are to be fitted by experiment to the model used to describe the system.

Using

$$\vec{S}_i = (-1)^i \vec{\phi} + \vec{\phi} \times \vec{\Pi} \quad (C7)$$

The boson Hamiltonian can now be written

$$H = \int dx \left[\frac{v}{2} \vec{\Pi}^2 + \frac{v}{2} \left(\frac{\partial \vec{\phi}}{\partial x} \right)^2 + \frac{1}{2v} \vec{\phi} \cdot \mathbf{D} \vec{\phi} - \mu_B \vec{H} \cdot \mathbf{G}(\vec{\phi} \times \vec{\Pi}) + \right. \\ \left. \frac{1}{v} \vec{\phi} \cdot \mathbf{d}(\vec{\phi} \times \vec{\Pi}) - \mu_B \vec{\phi} \cdot \mathbf{g} \vec{H} + \lambda(\vec{\phi}^2)^2 \right] \quad (\text{C8})$$

The term containing \mathbf{d} breaks the Z_2 symmetry along the a' (lowest mass) direction. It will also renormalize the masses. The second effect can be ignored in the approximation that the ϕ^4 term is ignored if we assume the masses are physical. The first effect leads to the presence of a static staggered field even below a critical magnetic field. A gap will always persist. The staggered field term will break the Z_2 symmetry along the c' or b axis, depending on whether the field is applied in the b or c' direction, respectively. A static staggered moment will likewise appear due to this term.

We would now like to discuss the effect of having two inequivalent chains per unit cell, with local axes different from the crystallographic axes. We label the two chains found in a unit cell of NENP ‘chain 1’ and ‘chain 2’ corresponding to the chains in the upper right and lower left corners of Figure 8 respectively. The dispersion branches of chain 1 are given by (20) of [7] only the field is $\alpha - 30^\circ$ from the c' axis where α is the angle of the field from the crystallographic c -axis. Similarly, the dispersion branches of chain 2 are calculated with the field $\alpha - 150^\circ$ from the c' axis. We can now graph these and compare with experiment.

Experiments which average over signals, like susceptibility or NMR T_1^{-1} measurements, must consider their results an average of two different experiments (corresponding to the two different chains with their relatively different field configurations). on the other hand, experiments such as ESR, should show a separate signal for each chain. The NMR relaxation calculations performed in the main part of the text ignore these effects. This ought not make a difference to the qualitative conclusions.

Figure 9 shows the dispersions for chains 1 and 2 (solid and dashed lines, respectively) when the field is $\pi/3$ from the crystallographic c axis in the ac -plane. This is an example of how transitions at two field strengths ought to be possible in the ESR experiment.

Figure 10 shows the resonance field versus orientation of field in the crystallographic ac -plane. The lower branch denotes transitions in chain 1 while the upper branch corresponds to transitions in chain 2. The transitions were calculated at .19 meV. corresponding to 47 GHz In addition the experimental results of Date and Kindo²⁰ are represented by the crosses. One immediately sees that the data does not compare well with the predictions based on the free model used above, for instead of following one of the branches, the experimental results lie between them. Furthermore, it seems unlikely that perturbations will cause such a significant shift in the resonance field. One sees that the discrepancy is $\sim \pm 1$ Tesla. One possible explanation is that since the ESR signal in [20] was also $\sim \pm 1$ Tesla in width and symmetric (in conflict with the predictions of [7]), the signal from the resonances in both chains was somehow smeared and interpreted as one single peak. Seen that way the model predictions are in good agreement except for the large field regime. One also has to keep in mind that the high-field boson dispersions are not accurate and therefore the predictions at larger angles could easily be .5 Tesla (or more) off the mark.

To end this discussion on, we'd like to elaborate on a previously made statement regarding the assignment of masses to the local Ni symmetry axes. It's easy to see that switching the masses around is tantamount to a $\pi/2$ shift in Figure 7 (the fact that the gyromagnetic

constants are not the same in orthogonal directions will not change the ESR resonance graph much since the ratio of the gyromagnetic constants is 0.98). Redrawing Figure 10 with this geometry misses the experimental results by 4 Tesla at 0 and 90 degrees, where the two chain resonances coincide. This determines the proper labeling of the local symmetry axes.

REFERENCES

- ¹ F.D.M. Haldane, Phys. Lett. **93A**, 464 (1983). For a review see I. Affleck, J. Phys.:Condensed Matter **1**, 2047 (1989).
- ² I. Affleck, Phys. Rev. B **41**, 6697 (1990).
- ³ A.M. Tsvelik, Phys. Rev. B **42**, 10499 (1990).
- ⁴ I. Affleck, Phys. Rev. B **43**, 3215 (1991).
- ⁵ I. Affleck and R.A. Weston, Phys. Rev. B **45**, 4667 (1992).
- ⁶ P. P. Mitra, B.I. Halperin and I. Affleck, Phys. Rev. B **45**, 5299 (1992).
- ⁷ I. Affleck, Phys. Rev. B **46**, 9002 (1992).
- ⁸ Th. Jolicoeur and O. Golinelli, Phys. Rev. B **50**, 9265, (1994).
- ⁹ N. Fujiwara et. al., Phys. Rev. B **47**, 11860 (1993).
- ¹⁰ I. Affleck, Phys. Rev. Lett. **56**, 746 (1986).
- ¹¹ E. S. Sørensen and I. Affleck, Phys. Rev. B **49**, 13235 (1994) and Phys. Rev. B **49**, 15771 (1994).
- ¹² P. P. Mitra and B.I. Halperin, Preprint.
- ¹³ S. Sachdev et. al., Phys. Rev. B **50**, 13006, 1994.
- ¹⁴ M. Troyer et. al., Phys. Rev. B **50**, 13515 (1994).
- ¹⁵ G.D. Mahan, *Many Particle Physics* (Plenum Press, 1993), p. 604.
- ¹⁶ M. Takigawa et. al., Preprint
- ¹⁷ J.L. Cardy, Nuc. Phys. **B270**, 186 (1986).
- ¹⁸ Jean-Paul Blaizot and Georges Ripka, *Quantum Theory of Finite Systems* (MIT Press, 1986), Chapter 3.
- ¹⁹ A. Meyer et. al., Inorg. Chem. **21**, 1729 (1982).
- ²⁰ M. Date and K. Kindo, Phys. Rev. Lett. **65**, 1659 (1990).

FIGURES

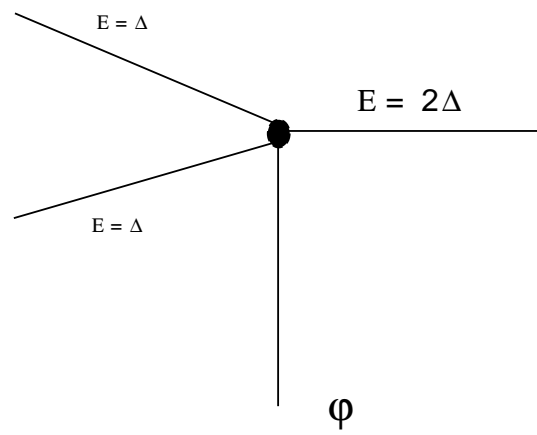


FIG. 1. First non-vanishing contribution to relaxation due to the staggered part of the spin

Magnon Dispersions For Lowest Two Branches

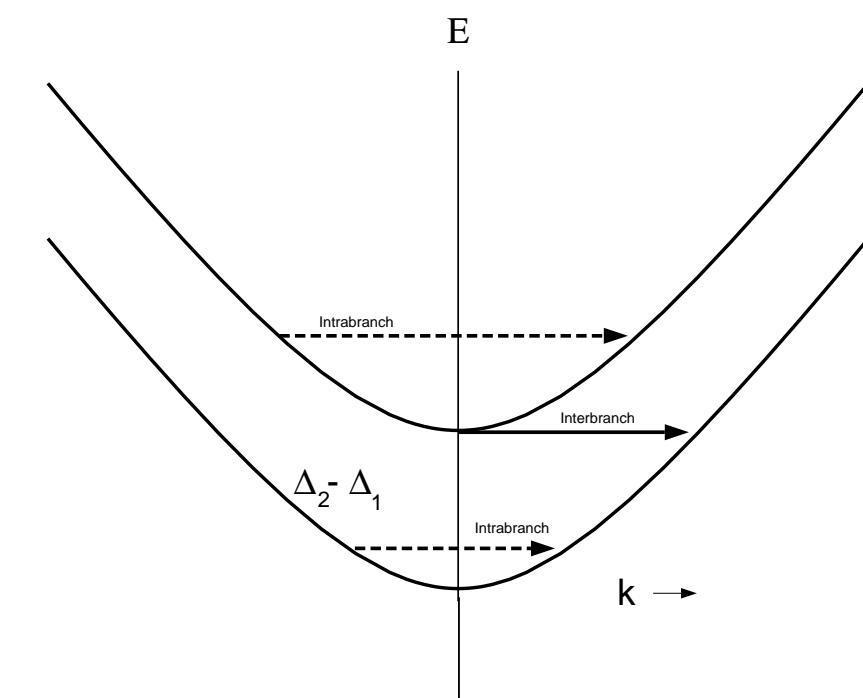


FIG. 2. Inter- vs Intraband transitions

Boson $F(H,T)$:

Contributions From The Uniform Part of the Spin

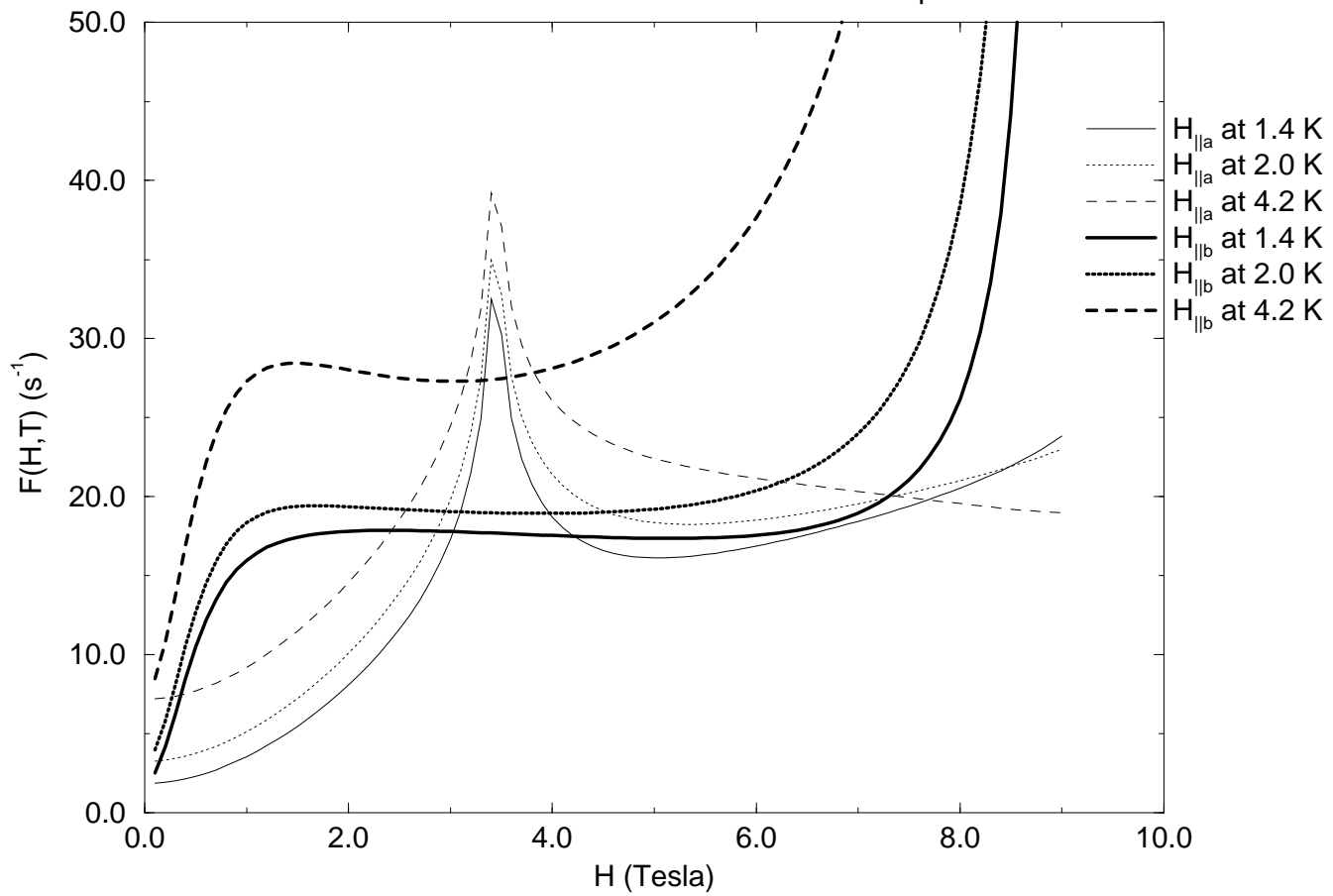


FIG. 3. $F(h,T)$ for bosons: field along crystal b and c directions

Boson $F(H,T)$:

Contributions From The Uniform Part of the Spin

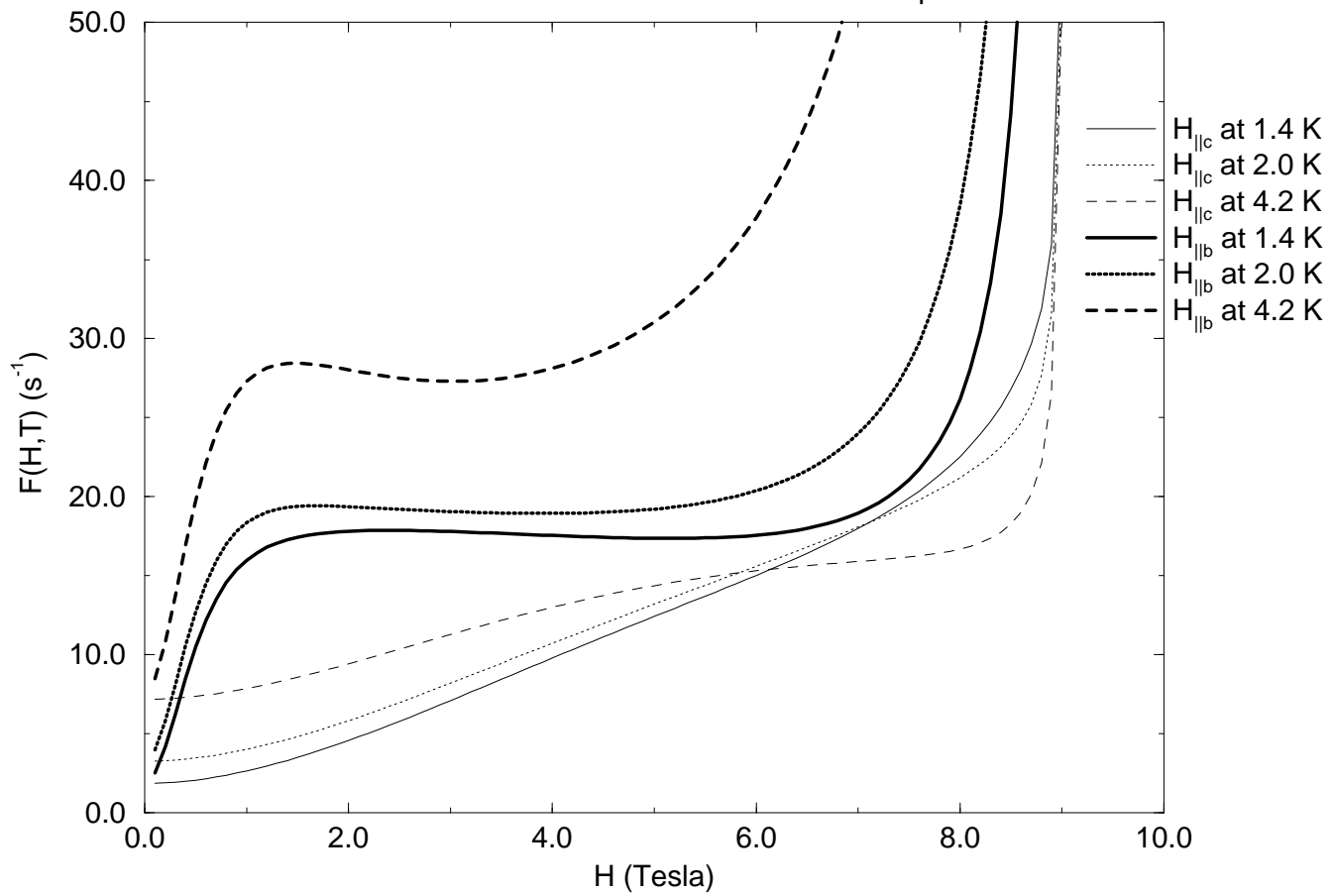
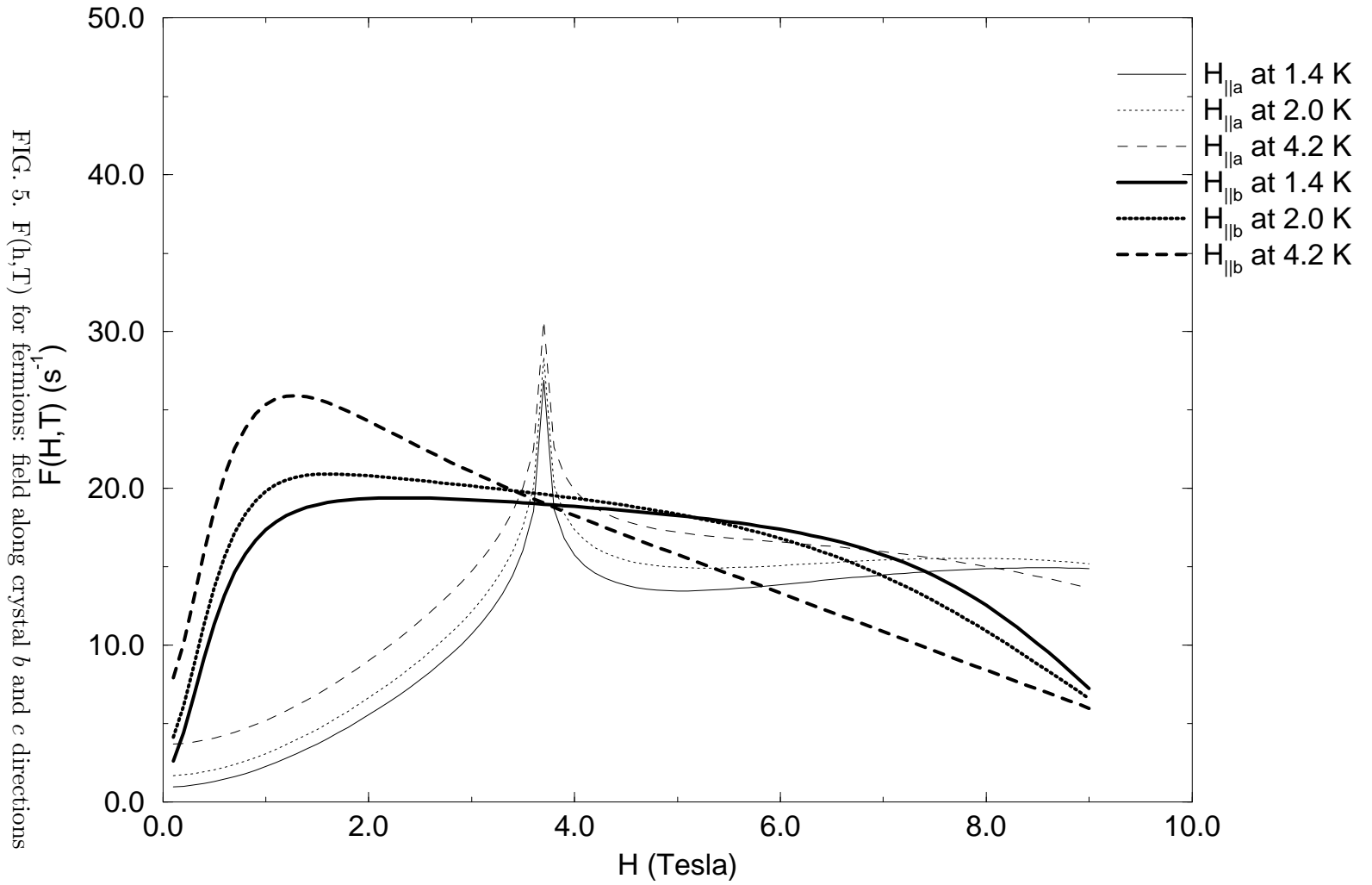


FIG. 4. $F(h,T)$ for bosons: field along crystal b and a directions

Fermion $F(H,T)$:

Contributions From The Uniform Part of the Spin



Fermion $F(H,T)$:

Contributions From The Uniform Part of the Spin

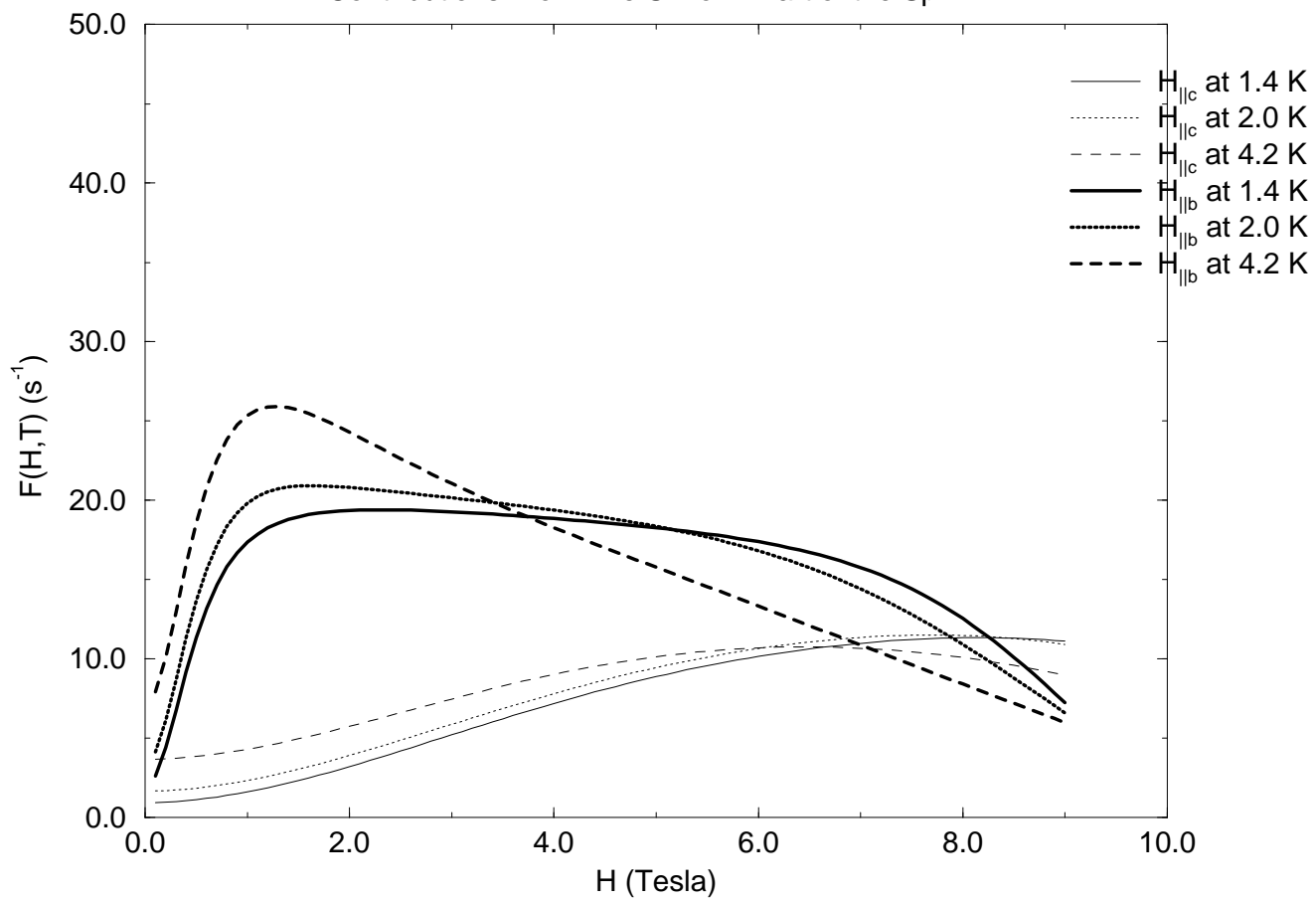


FIG. 6. $F(h,T)$ for fermions: field along crystal b and a directions

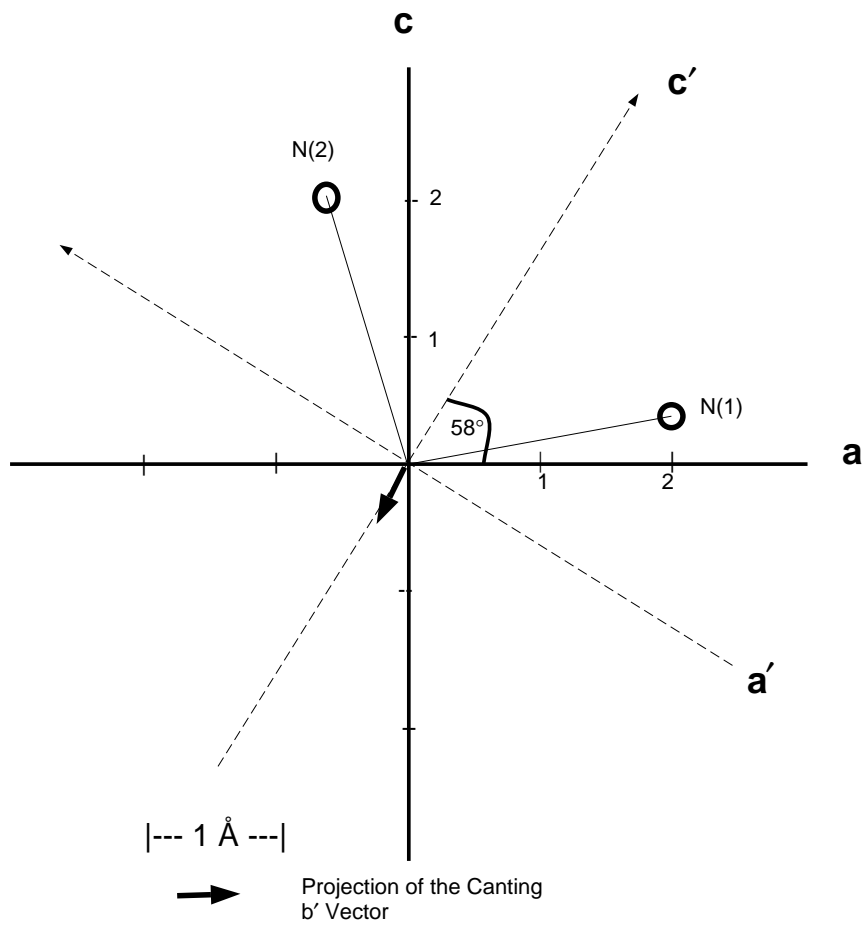


FIG. 7. Local and crystallographic axes projected onto the ac -plane in NENP

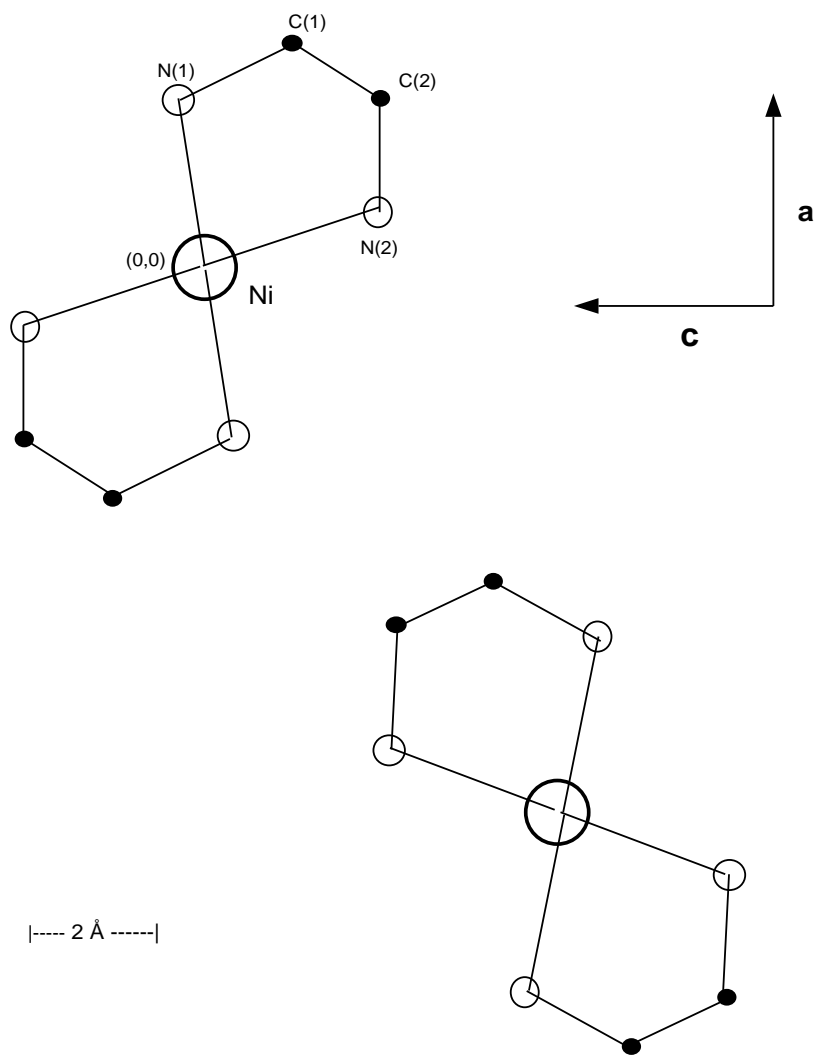


FIG. 8. A projection of the NENP unit cell onto the ac -plane showing two chains per unit cell

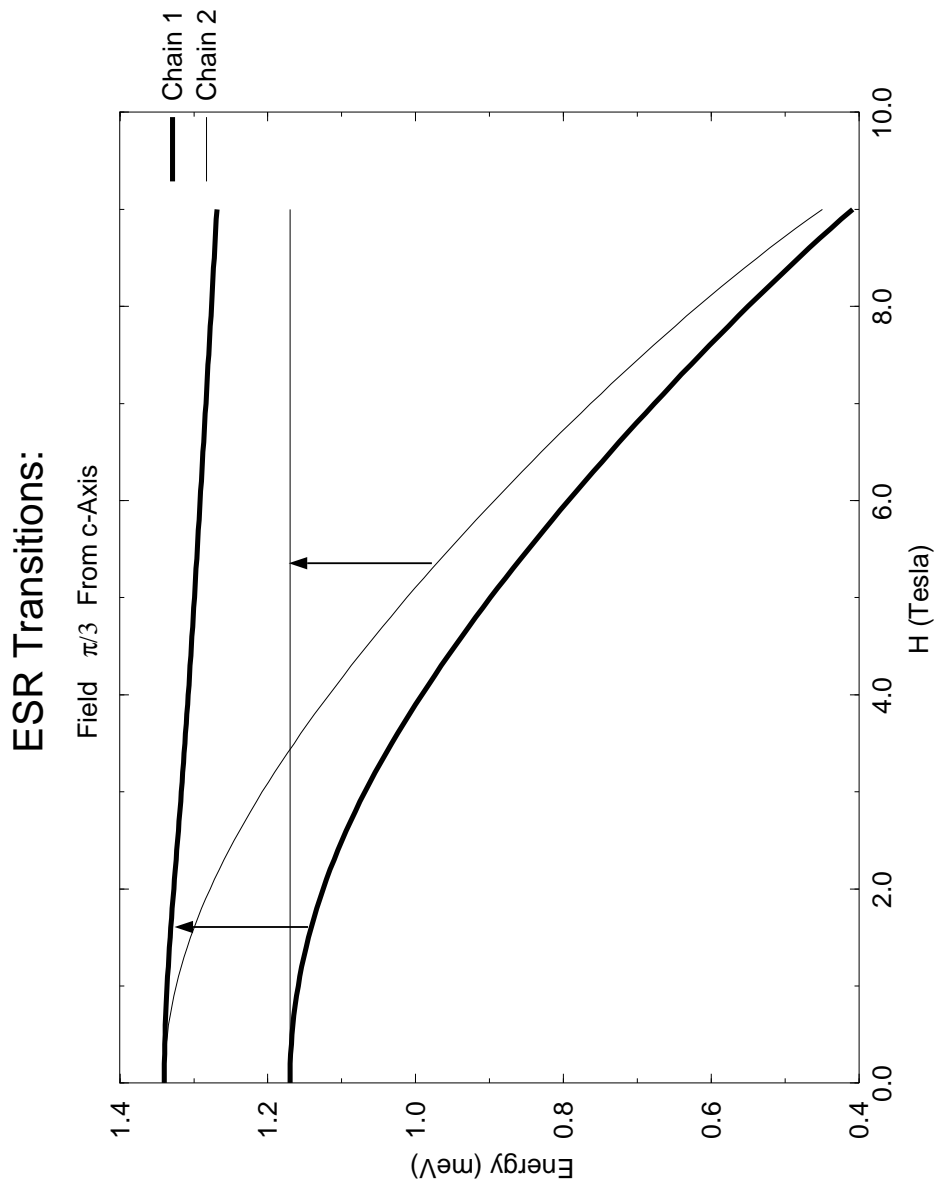


FIG. 9. Dispersions for the two chain conformations and sample resonant transitions for a uniform field placed 60° from the crystallographic c -axis.

ESR Resonance in NENP

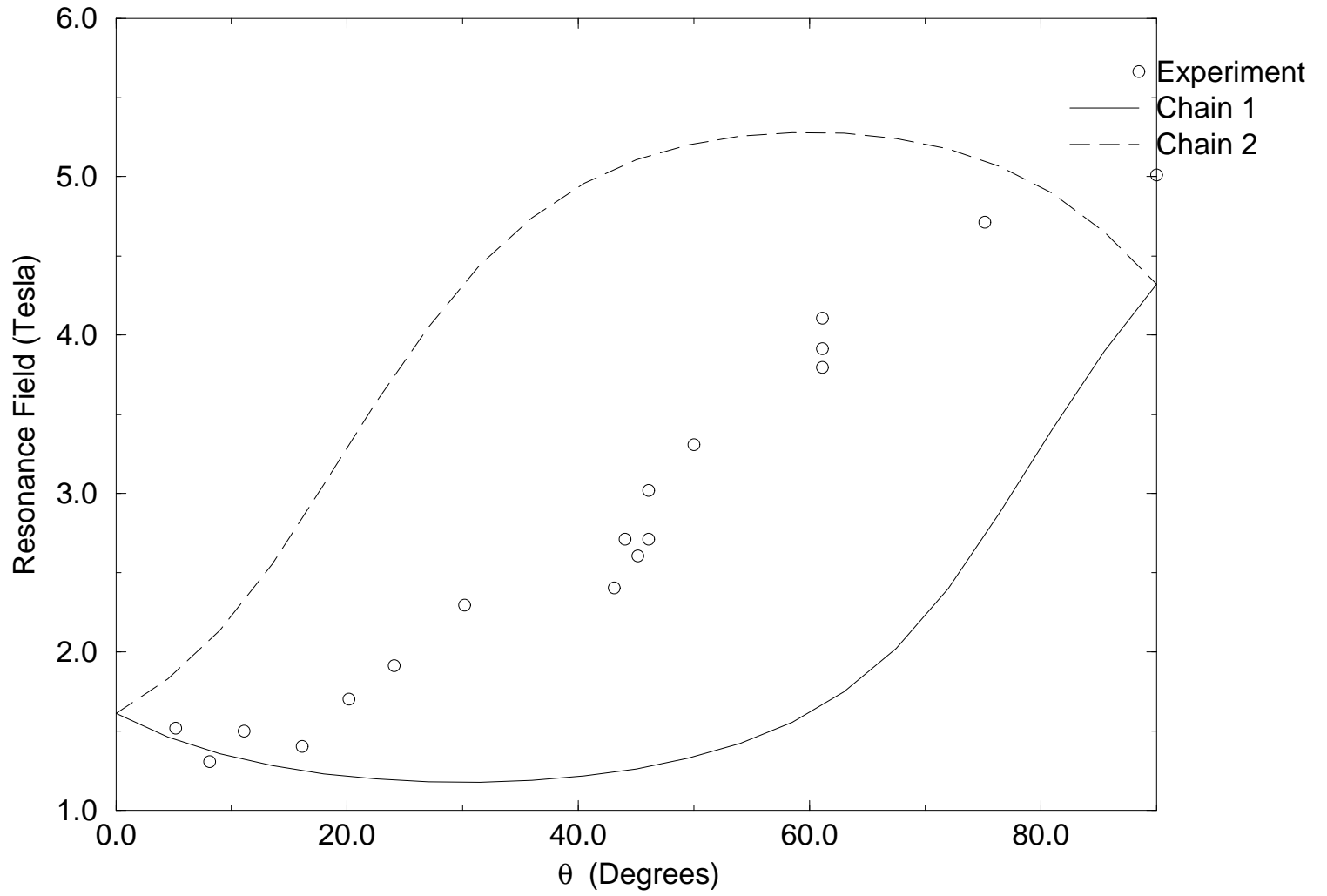


FIG. 10. Resonant field vs. field orientation in the ac -plane for .19 meV transitions.